Circulating CXCR5[superscript +]CXCR3[superscript +]PD-1[superscript lo] Tfh-like cells in HIV-1 controllers with neutralizing antibody breadth

Circulating CXCR5^{+}CXCR3^{+}PD-1^{Lo} Tfh-like cells in HIV-1 controllers with neutralizing antibody breadth

Enrique Martin-Gayo[1], Jacqueline Cronin[1], Taylor Hickman[1], Zhengyu Ouyang[1], Madelene Lindqvist[1,2], Kellie E. Kolb[1,3], Julian Schulze zur Wiesch[4], Rafael Cubas[5], Filippos Porichis[1], Alex K. Shalek[1,3], Jan van Lunzen[4], Elias K. Haddad[6], Bruce D. Walker[1,2,7], Daniel E. Kaufmann[1,2,8], Mathias Lichterfeld[1,9] and Xu G. Yu[1].

[1] Ragon Institute of MGH, MIT and Harvard, Cambridge, MA

[2]Center for HIV/AIDS Vaccine Immunology and Immunogen Discovery (CHAVI-ID)

[3] MIT Institute for Medical Engineering & Science (IMES) and Chemistry, Cambridge, MA

[4] University Medical Center Hamburg, Hamburg, Germany

[5] Vaccine & Gene Therapy Institute of Florida, Port St. Lucie, FL

[6]Drexel University, Division of Infectious Diseases and HIV Medicine, Philadelphia, PA

[7] Howard Hughes Medical Institute, Chevy Chase, MD, USA

[8] CHUM Research Center, University of Montreal, Montreal, Quebec, Canada

[9] Infectious Disease Divisions, Brigham and Women's Hospital and Massachusetts General Hospital, Boston, MA

Corresponding author:
Xu G. Yu, M. D.
Associate Professor of Medicine
Ragon Institute of MGH, MIT and Harvard

Massachusetts General Hospital
400 Technology Square
Cambridge, MA 02139, USA
Phone: 857-268-7004
e-mail: xyu@mgh.harvard.edu

Conflict of interest statement

The authors have declared that no conflict of interest exists.

Abstract

HIV-1-specific broadly-neutralizing antibodies (bnAbs) typically develop in individuals with continuous high-level viral replication and increased immune activation, conditions that cannot be reproduced during prophylactic immunization. Understanding mechanisms supporting bnAb development in the absence of high-level viremia may be important for designing bnAb-inducing immunogens. Here, we show that the breadth of neutralizing antibody responses in HIV-1 controllers was associated with a relative enrichment of circulating CXCR5^{+} CXCR3^{+} PD-1^{Lo} CD4 T cells. These CXCR3^{+} PD-1^{Lo} Tfh-like cells were preferentially induced *in vitro* by functionally superior dendritic cells from controller neutralizers, and able to secrete IL-21 and support B cells. In addition, these CXCR3^{+} PD-1^{Lo} Tfh-like cells contained higher proportions of stem cell-like memory T cells, and upon antigenic stimulation differentiated into PD-1^{Hi} Tfh-like cells in a Notch-dependent manner. Together, these data suggest that CXCR5^{+} CXCR3^{+} PD-1^{Lo} cells represent a dendritic cell-primed precursor cell population for PD-1^{Hi} Tfh-like cells that may contribute to the generation of bnAbs in the absence of high-level viremia.

Introduction

Antibodies with broad neutralizing activity against different strains of HIV-1 (bnAbs) (1,2), represent immune responses that in principle, could be reproduced in healthy individuals to prevent infection with HIV-1. However, mechanisms required to generate and maintain such bnAbs seem extremely complex, and remain poorly understood. Follicular $CD4^+$ T helper cells (Tfh) are critical for priming of B cell responses within lymph node germinal centers that leads to the development of bnAbs (3,4). Tfh cells are phenotypically characterized by the expression of the surface receptor CXCR5, and their developmental program is regulated by the master transcription factor Bcl-6 (5,6). Functionally, Tfh cells enhance maturation, immunoglobulin class-switching and affinity maturation in B cells by secreting cytokines such as IL-21 and IL-4 (7,8), and through contact-dependent mechanisms (9,10). The molecular and cellular signals necessary for Tfh development represent an area of active investigation, but current data from experimental animal models suggest that antigen presentation by dendritic cells (DC) is necessary and sufficient to initiate a Tfh development program (11,12), while cognate interactions with activated B cells seem required to sustain dendritic cell-primed Tfh cells (13).

Tfh cells reside in lymphoid tissue (14), but a population of $CXCR5^+$ $PD\text{-}1^+$ $CD4^+$ T lymphocytes circulating in the peripheral blood has been proposed to act as peripheral counterparts of Tfh cells (pTfh) (15,16). In comparison to germinal center Tfh, peripheral blood $CXCR5^+$ CD4 T cells express reduced levels of ICOS, Bcl-6 and cellular activation markers such as CD69 and HLA-DR, but maintain the ability to stimulate Ab production and Ig class switching in B cells *in vitro* upon reactivation with cognate antigens (15,17), suggesting that they represent Tfh-committed memory cells. pTfh cells have been further subdivided into distinct subsets based on expression of CXCR3 and CCR6 receptors, but the contribution of each subtype to the development of humoral immunity remains controversial (16-19). In HIV-1 infection, associations between circulating $CXCR5^+$ $CXCR3^-$ $PD\text{-}1^+$ Tfh and the breadth of HIV-1-specific neutralizing antibodies were made in a cohort of

chronically infected individuals with continuously-ongoing high plasma viral loads and high immune activation (16). In contrast, following immunization with Influenza vaccines (19) or Human Papilloma-Virus (HPV) vaccines (20) (i. e. during more limited antigen exposure), humoral immune responses were correlated with CXCR3^{+} CXCR5^{+} PD-1^{+} CD4 T cells, and CXCR3^{+} CXCR5^{+} CD4 T cells were also observed in blood and lymph nodes in rhesus macaques immunized with an SIV vaccine (21). In addition, recent studies in non-human primate models also reported induction of CXCR3^{+} Tfh in chronic SIV infection (22). Therefore, the contribution of pTfh subsets to the development of protective Ab responses seems to be context-dependent, and requires further investigation.

HIV-1 controllers are able to spontaneously maintain low or undetectable levels of viral replication, and arguably provide the most informative opportunity to study effective HIV-1 immune defense mechanisms. Most prior studies in these patients have focused on cellular mechanisms of antiviral immune control, and identified highly-functional HIV-1-specific memory CD4 and CD8 T cell responses as the predominant correlate of antiviral immune defense (23); this represents a sharp contrast to HIV-1 progressors in whom there is considerable evidence for a defective and functionally-exhausted memory cell response to HIV-1. Mechanisms of HIV-1-specific humoral immunity and memory pTfh cells in HIV-1 controllers remain largely uncertain, although prior studies noted that the development of HIV-1-specific antibodies with increased neutralizing breadth seems rare in these patients (24). In the present study, we show that relative enrichment of CXCR5^{+} CXCR3^{+} PD-1^{Lo} CD4 T cells is associated with increased HIV-1 neutralizing antibody breadth in controllers. Importantly, CXCR3^{+} PD-1^{Lo} Tfh-like cells were efficiently primed by myeloid DC (mDC) from HIV-1 controller neutralizers, were phenotypically enriched for immature, stem cell-like CD4 T cells, and were able to partially support B cell differentiation and secreted high levels of IL-21 upon antigen stimulation, suggesting they might contribute to humoral responses in these patients.

Results

Ratios of circulating PD-1^{Lo}/PD-1^{Hi} CXCR3^{+} Tfh-like cells correlate with neutralizing antibody breadth in controllers.

Circulating CXCR5^{+} CD4 T cells can be classified into CXCR3^{+} and CXCR3^{-} subsets (Supplemental Figure 1A). In untreated HIV-1 patients with progressive disease, evolution of broadly-neutralizing antibody responses has been associated with proportions of circulating CXCR5^{+} CXCR3^{-} PD-1^{+} Tfh-like cells, which seem to represent the peripheral counterpart of conventional Tfh located in lymphoid tissues and are therefore termed pTfh [16]. However, cellular immune responses supporting bnAbs evolution under conditions of limited antigen exposure are unknown. To address this, we selected a cohort of controllers who spontaneously maintained HIV-1 replication levels of less than 1500 copies/ml and further subdivided them into two groups based on the presence (neutralizers) or the absence (non-neutralizers) of antibodies with neutralizing activity against Tier-2 HIV-1 viruses in plasma, with no significant difference in viral loads, CD4 counts and HLA allele distributions (Supplemental Table 1 and 2). We found that in HIV-1 controller neutralizers, the proportions of CXCR5^{+} CXCR3^{-} PD-1^{+} pTfh were significantly lower than the proportions of CXCR5^{+} CXCR3^{+} PD-1^{+} CD4 T cells (Figure 1A). In addition, in contrast to prior studies in HIV-1 progressors (16), the proportions of CXCR5^{+} CXCR3^{-} PD-1^{+} pTfh were not associated with the breadth of neutralizing antibodies in controllers ($p=0.49$, $R=0.14$). Similarly, proportions of CXCR5^{+} CXCR3^{+} PD-1^{+} cells were also unrelated to neutralizing antibody breadth in this patient population ($p=0.76$, $R=0.06$). Based on the intensity of PD-1 surface expression, we further classified circulating CXCR5^{+} T cells into PD-1^{Hi} and PD-1^{Lo} cells (Supplemental Figure 1B), as previously suggested (16). Interestingly, we found that proportions of both CXCR3^{+} and CXCR3^{-} PD-1^{Lo} cells in the peripheral blood were higher in controller neutralizers compared to controller non-neutralizers, while CXCR3^{+} and CXCR3^{-} PD-1^{Hi} cell subsets were not different between these two patient populations (Figure 1B). Yet, neither proportions of PD-1^{Lo} nor PD-1^{Hi} CXCR5^{+} CD4 T cells were associated with neutralizing antibody

breadth in controller neutralizers, independently of CXCR3 expression (data not shown). In contrast, the ratios between PD-1^{Lo} and PD-1^{Hi} cells within CXCR5^{+} CXCR3^{+} T cells were positively correlated with the breadth of the HIV-1-specific neutralizing antibody responses (Figure 1C, nominal p=0.02) in controller neutralizers. These associations seemed to be specific of the CXCR5^{+} CXCR3^{+} CD4 T cell compartment, since the ratio of PD-1^{Lo} *vs.* PD-1^{Hi} cells within the CXCR5^{+} CXCR3^{-} CD4 T cell populations was unrelated to neutralizing antibody breadth (Figure 1C). Together, our data indicate that enrichment of CXCR5^{+} CXCR3^{+} PD-1^{Lo} relative to CXCR5^{+} CXCR3^{+} PD-1^{Hi} Tfh-like cells in blood is associated with the breadth of neutralizing antibodies in the absence of high-level HIV-1 replication.

Primary myeloid dendritic cells from HIV-1 controller neutralizers preferentially prime naïve CD4 T cells into PD-1^{Lo} Tfh-like cells.

A number of experimental animal studies suggest that dendritic cells are indispensable for initiating a Tfh development program in naïve CD4 T cells (11,12). Therefore, we hypothesized that the relative enrichment of PD-1^{Lo} *vs.* PD-1^{Hi} CXCR3^{+} Tfh-like cells in the blood from controller neutralizers might be associated with differential priming by DCs. To evaluate the ability of human myeloid DCs (mDC) to polarize CD4 T cells towards Tfh lineage commitment *in vitro*, we established a co-culture system with autologous naïve CD4 T cells and naïve B cells from HIV-1 negative individuals in the presence or absence of primary mDC isolated from the blood of an allogeneic healthy donor, without addition of exogenous antigens. After 7 days of co-culture, maturation of naïve CD4 T cells into cells with a Tfh-like phenotype was analyzed by flow cytometry. As shown in Figure 2A, and consistent with previous studies (25), CD4 T cells were unable to efficiently upregulate the expression of the Tfh markers, CXCR5 and PD-1, when cultured in media or in the presence of naïve B cells alone. However, when mDC were added to the co-culture, a significant proportion of CXCR5^{+} PD-1^{+} T cells was detected on day 7 of culture (Figure 2A), suggesting *de novo* differentiation of naïve CD4 T cells into Tfh-like cells

in vitro. Similarly to cells from peripheral blood, CXCR5^{+} T cells induced in this assay could also be subdivided into PD-1 ^{Lo} and PD-1 ^{Hi} subpopulations (Figure 2A). Further phenotypical analysis revealed that both PD-1 ^{Lo} and PD-1 ^{Hi} CXCR5^{+} T cells also expressed additional Tfh markers such as Bcl-6 and ICOS (26,27) (Figure 2B and Supplemental Figure 2A), while expression of FoxP3, a marker for follicular regulatory T cells (Tfr) (28), was low (Supplemental Figure 2A). Of note, most DC-primed CXCR5^{+} PD-1^{+} T cells expressed the chemokine receptor CXCR3 (Supplemental Figure 2A). To examine whether the primed T cells generated in our co-culture system were more similar to Th1 or Tfh1 cells, we analyzed intracellular expression levels of the Th1 transcription factor Tbet (29). As shown in Supplemental Figure 2A-2B, Tbet was detected in CXCR5^{+} PD-1^{+} T cells, but levels of expression were much lower than in bona fide Th1 cells primed with LPS-pulsed mDC (Supplemental Figure 2B). Therefore, our data indicate that human primary mDC are required to efficiently prime naïve CD4 T cells into CXCR5^{+} PD-1^{+} Tfh1-like cells in the presence of B cells *in vitro*. Importantly, *in vitro* generation of CXCR3^{+} ICOS^{+} PD-1^{Lo} and PD-1^{Hi} Tfh1-like cells was also observed in the presence of primary mDC isolated from lymph node biopsies from HIV-1 negative donors (Supplemental Figure 2C).

Using this experimental system, we next determined the ability of mDC from different cohorts of HIV-1-infected individuals to prime Tfh-like cells *in vitro*. To this end, we evaluated the Tfh-priming potential of mDC from controller neutralizers (NT) and non-neutralizers (NN), Viremic (CP) and HAART-treated (H) chronically HIV-1-infected individuals. A cohort of HIV-1 negative persons (NG) was also included for comparative purposes. Subsequently, mDC were isolated from all study groups and their *in vitro* Tfh priming abilities were tested by co-culture assays using identical allogeneic naïve CD4 T and B cells from HIV-1 negative donors. As shown in Figure 2C, generation of PD-1^{Hi} Tfh-like cells was less efficient in the presence of mDC from HIV-1 infected donors, compared to uninfected individuals, but mDC from controller neutralizers and non-neutralizers seemed equally effective in inducing cells with a PD-1^{Hi} Tfh phenotype. However, mDC from controller neutralizers

induced higher proportions of PD-1^{Lo} Tfh-like cells compared to controller non-neutralizers and chronically infected, viremic or HAART-treated individuals (Figure 2C). Notably, the ratios of PD-1^{Lo} *vs.* PD-1^{Hi} Tfh-like cells generated in the presence of mDC from controller neutralizers were higher than in assays with mDC from all other study cohorts, and significantly exceeded the ratios of PD-1^{Lo} *vs.* PD-1^{Hi} cells generated in the presence of healthy individuals (Figure 2D). Notably, preferential induction of CXCR5^{+} PD-1^{Lo} T cells by mDC from HIV-1 controller neutralizers was not associated with significantly higher levels of specific cytokines (Supplemental Figure 2D), despite a tendency for higher detection of IL-6, IL-10 and IL-21. Similarly, cultures performed with mDC from controller neutralizers did not show specific phenotypic alterations in co-cultured B cells (Supplemental Figure 3A-3B), or significant changes in the immunoglobulin (Ig) classes secreted by B cells (Supplemental Figure 3C). However, the contribution of class G Ig to the total amount of secreted Ig was highest in assays with mDC from controller neutralizers (Supplemental Figure 3C). Together, these data indicate that primary mDC from controller neutralizers have superior abilities to prime PD-1 ^{Lo} CXCR3^{+} CXCR5^{+} Tfh-like cells *in vitro*, compared to mDC from controller non-neutralizers.

Distinct transcriptional signatures in mDC from controller neutralizers

To better understand molecular mechanisms underlying enhanced abilities of mDC from controller neutralizers to prime Tfh-like cells, we analyzed transcriptional profiles of mDC from 4 controller neutralizers compared to cells from 4 controller non-neutralizers. These analyses revealed significant differences (FDR-adjusted $p<0.05$) in the expression of 930 genes in mDC from controller neutralizers (Figure 3A, Supplemental Table 3), as determined by DESeq2 (30). Overall, pathways upregulated in controller neutralizers shared a high number of genes with interconnected functions in innate and adaptive immunity, consistent with the diverse role of DC in orchestrating antiviral immune defense (Figure 3B). Interestingly, we observed that pathways previously associated with Tfh priming, such as ICOSL-ICOS interactions ($p=3.98x10^{-11}$) and CD40-dependent signaling ($p=0.00079$) (31) (Figure 3B), were enriched in transcriptional signatures of mDC

from controller neutralizers. In addition, genes encoding for signaling components of the IL-6 ($p=0.001$) and IL-1 ($p=9.54x10^{-6}$) pathways, critical for functional development of Tfh cells and the inhibition of alternative T helper cell lineages (32,33), were also significantly upregulated in mDC from controller neutralizers (Figure 3B), as were transcripts involved in general DC maturation and activation, features of mDC previously involved in improved Tfh generation (34). Consistent with these observations, biocomputational analysis identified signaling through CD40 ($p=1.05x10^{-23}$) or CD86 ($p=5.05x10^{-10}$), secretion of multiple effector cytokines such as IFNα ($p=3.98x10^{-26}$), TNFα(1.96×10^{-16}), IL-1β ($p=4.55 \times 10^{-13}$), IL-6 ($p=3.2x10^{-11}$), IL-10 ($p=4.5x10^{-15}$) and IL-18 ($p=2.89x10^{-17}$) (Figure 3C), and transcription factors and signal mediators such as NFKB1 ($p=5.88x10^{-16}$), STAT3 ($p=9.47x10^{-15}$), IRAK4 ($p=7.45x10^{-13}$) and ID3 ($p=3.97x10^{-21}$) as putative upstream regulators of transcriptional signatures in mDC from controller neutralizers (Figure 3C-D). In contrast, transcriptional pathways down-regulated in DC from controller neutralizers had no immediate connection to Tfh priming and DC function (Figure 3B). To further explore these observations, we performed functional *in vitro* co-culture assays between DC and T/B cells using a trans-well experimental system. As previously described for CXCR5^{+} CXCR3^{-} PD-1^{+} cells (31,35), *in vitro* priming of CXCR3^{+} CXCR5^{+} PD-1^{Lo} Tfh-like cells seemed to require direct contact with mDC (Supplemental Figure 4A). Flow cytometry analysis revealed that among all costimulatory molecules tested, ICOS-L and more significantly CD40 tended to be expressed at higher levels on mDC from controller neutralizers (Figure 3E, Supplemental Figure 4B), consistent with the described transcriptional profiling experiments. Importantly, inhibition of cellular communication via CD40/CD40L (Figure 3F) significantly abrogated the priming of Tfh-like cells by mDC, although such interactions alone did not explain the preferential induction of PD-1^{Lo} by mDC from controller neutralizers. Collectively, these data indicate that mDC from controller neutralizers are characterized by transcriptional signatures associated with key pathways involved in Tfh priming.

CXCR5^{+} CXCR3^{+} PD-1^{Lo} CD4 T cells are detectable in lymphoid tissues in vivo.

We next investigated the presence of CXCR5^{+} CXCR3^{+} PD-1^{Lo} Tfh-like cells in peripheral blood and tissue samples isolated directly *ex vivo* in samples from HIV-1-negative persons (Supplemental Figure 1A-1B). We found that similarly to peripheral blood, the proportions of CXCR5^{+} CXCR3^{+} CD4 T cells approximated those of CXCR5^{+} CXCR3^{-} CD4 T cells in the lymph node, and that the majority of CXCR5^{+} CD4 T cells in these tissues were PD-1^{Lo}, independently of CXCR3 co-expression (Supplemental Figure 1A-1B). In contrast, in tonsil tissue, PD-1^{Lo} cells were mostly detected in CXCR5^{+} CXCR3^{+} cells, while CXCR5^{+} CXCR3^{-} CD4 T cells consisted almost entirely of PD-1^{Hi} cells. Notably, CXCR3^{-} PD-1^{Hi} cells were the dominant cell subset within CXCR5^{+} lymphocytes in tonsils, while CXCR3^{+} PD-1^{Lo} cells represented the largest cell compartment within CXCR5^{+} CD4 T cells from blood and lymph nodes (Supplemental Figure 1B). Moreover, within lymph nodes and tonsils, Bcl-6 was upregulated in all CXCR5^{+} CD4 T cells, irrespective of their CXCR3 or PD-1 expression levels, as opposed to CXCR5^{+} CD4 T cells from peripheral blood, in which Bcl-6 levels were very low and indistinguishable from those of total CD4 T cells, consistent with prior results (3) (Supplemental Figure 5). ICOS was more strongly expressed in PD-1^{Hi} Tfh-like cells compared to PD-1^{Lo} cells across all tissues (Supplemental Figure 5). Together, our data indicate that CXCR5^{+} CXCR3^{+} PD-1^{Lo} cells are present *in vivo* in lymphoid tissues.

CXCR3^{+} PD-1^{Lo} Tfh-like cells support B cell activation and differentiation.

Previous studies defined CXCR3^{+} pTfh as poor supporters of B cell maturation based on their weak ability to stimulate class switching to IgG in B cells *in vitro* (15,16). However, our results suggest that the presence of CXCR3^{+} PD-1^{Lo} Tfh-like cells might be beneficial for the development of neutralizing Abs against HIV-1 in controllers. To better understand the functional characteristics of CXCR3^{+} PD-1^{Lo} Tfh-like cells, different pTfh cell subsets from the blood of HIV negative individuals (Supplemental Figure 1A-1B) were sorted and cultured with autologous total B cells in the presence of staphylococcal endotoxin B (SEB). After 6 days of culture, differentiation

of pTfh subsets, maturation of B cells, cytokine secretion profiles and levels of secreted immunoglobulins were analyzed. As shown in Figure 4A-4B, most CXCR3^{+} and CXCR3^{-} CXCR5^{+} PD-1^{Lo} Tfh-like cells differentiated into PD-1^{Hi} Tfh-like cells in the presence of antigens and autologous B cells; however, some of the CXCR3^{+} and CXCR3^{-} PD-1^{Lo} Tfh-like cells seemed to be able to retain their original PD-1^{Lo} phenotype during co-culture (Figure 4A, 4C). In addition, significant levels of proliferation were detected on all subsets of pTfh cells present on day 6 of culture (Supplemental Figure 8A). Co-culture of B cells with any of the pTfh cell subsets was accompanied by a tendency for decreased proportions of resting memory B cells (Figure 4D, Supplemental Figure 6A), and a marked upregulation of CD38 and CD27, leading to elevated frequencies of CD38^{Int} CD27^{Int} activated memory B cells, CD38^{Hi} CD27^{Hi} plasmablast-like B cells (Figure 4D-4E) and CD38^{Hi} CD27^{-} transitional B cells (Supplemental Figure 6A). Notably, PD-1^{Lo} pTfh tended to be more efficient than PD-1^{Hi} cells in inducing activated memory B cells (Figure 4E). Overall, PD-1^{Lo} and PD-1^{Hi} CXCR3^{+} pTfh cells were able to induce comparable level of phenotypic maturation in B cells as CXCR3^{-} pTfh subsets. Interestingly, PD-1^{Lo} CXCR3^{+} pTfh seemed to secrete higher levels of IL-21 and, more significantly, of GM-CSF, IL-6 and IL-10 in a six-day co-culture assay with total B cells and SEB (Figure 4F and Supplemental Figure 6B). In agreement with previous studies, only CXCR3^{-} pTfh were able to efficiently induce full class switching to IgG in B cells, dominated by IgG1 (Figure 4G, Supplemental Figure 6C) (16-18). In contrast, PD-1^{Lo} and PD-1^{Hi} CXCR3^{+} cells seemed capable of stimulating B cells to produce IgM and IgA, IgG3 but not IgG1, as previously reported (16-18), suggesting a more limited ability of these pTfh subsets to support Ig class switching to IgG in our six-day co-culture assays (Figure 4G). Together, these data indicate that both CXCR3^{+} and CXCR3^{-} PD-1^{Lo} pTfh subsets mature into PD-1^{Hi} cells upon Ag stimulation, and that CXCR3^{+} pTfh cells display distinct, but partially overlapping functional abilities to support B cells compared to conventional CXCR3^{-} pTfh. These findings suggest that both CXCR3^{+} and CXCR3^{-} pTfh might participate in the development of Ab breadth at different levels.

CXCR3^{+} PD-1^{Lo} pTfh differentiate into PD-1^{Hi} cells in a Notch-dependent fashion.

While most PD-1^{Lo} Tfh-like cells differentiated into PD-1^{Hi} upon antigenic stimulation, we observed a small proportion of PD-1^{Lo} Tfh-like cells that were able to retain their original CXCR5^{+} PD-1^{Lo} phenotype during co-culture with B cells and SEB, suggesting self-renewal or homeostatic proliferation. To test this possibility, we first analyzed the expression of memory cell markers (Figure 5A-5B) on different Tfh-like subsets from human blood and lymphoid tissues. As shown in Figure 5C, PD-1^{Lo} and PD-1^{Hi} cells from both CXCR3^{+} and CXCR3^{-} peripheral Tfh were dominated by CCR7^{+} CD45RO^{+} central-memory T cells; in contrast, total CD4 T cells were dominated by naïve cells. In tonsils and lymph nodes, CXCR5^{+} CXCR3^{+} PD-1^{Lo} CD4 T cells also preferentially exhibited a central-memory phenotype, while PD-1^{Hi} cells, specifically within the CXCR3^{-} T cell pools, included higher proportions of CCR7^{-} CD45RO^{+} effector-memory cells (Figure 5C). Importantly, we observed that PD-1^{Hi} cells from all tissue compartments consisted mostly of CD45RO^{+} cells, while both CXCR3^{+} and CXCR3^{-} PD-1^{Lo} Tfh populations contained larger and more distinct populations of CD45RO^{-} naïve (NA)-like cells (Figure 5B). Subsequent experiments demonstrated that many of these CD45RO^{-} Tfh expressed CD95, a memory cell marker that when expressed on otherwise naïve-appearing CD4 T cells defines a highly immature population of extremely long-lived memory CD4 T cells with stem cell-like properties (Figure 5B) (36). In fact, in contrast to total CD4 T cells (Figure 5D), a large proportion of NA-like cells present in the different CXCR5^{+} subsets from the analyzed tissue compartments exhibited a CD95^{+} T stem cell memory phenotype, and the relative proportions of these CD45RO^{-} CD95^{+} cells tended to be higher within the PD-1^{Lo} populations (Figure 5D). Importantly, a similar memory subset distribution was observed between circulating Tfh-like cell populations from HIV-1 controller neutralizers and non-neutralizers (Supplemental Figure 7A). Interestingly, frequencies of stem cell-memory T cells within the CXCR3^{+} PD-1^{Lo} cell populations appeared to be increased in HIV-1 controller neutralizers (Supplemental Figure 7B). Therefore, CXCR5^{+} PD-1^{Lo} CD4 T cells seemed to contain higher proportions of more immature stem cell-memory T cells.

To investigate stem cell-like precursor properties of PD-1^{Lo} Tfh-like cells, we analyzed the developmental fate of CXCR5^{+} CXCR3^{+} PD-1^{Lo} in serial co-culture experiments. For this purpose, CXCR5^{+} CXCR3^{+} PD-1^{Lo} cells that maintained their original phenotype during an initial six-day co-culture assay with B cells and SEB were sorted and exposed to six additional days of culture with B cells and SEB. Interestingly, a considerable proportion of sorted CXCR5^{+} CXCR3^{+} PD-1^{Lo} CD4 T cells that remained PD-1^{Lo} during the initial culture also retained their original phenotype (Figure 6A-6B) during secondary culture, although a proportion of these cells was able to differentiate into PD-1^{Hi} cells (Figure 6A-6B). In contrast, the phenotype of sorted PD-1^{Hi} pTfh remained unchanged after the primary and secondary cultures, independently of CXCR3 expression (Figure 6B). Importantly, cells capable of maintaining a PD-1^{Lo} phenotype during primary (Supplemental Figure 8B-8C) and secondary cultures (Supplemental Figure 8D) showed signs of active proliferation. This suggests that even though the majority of PD-1^{Lo} CXCR5^{+} cells ultimately transition to PD-1^{Hi} cells, a proportion of these cells appear to maintain their original phenotype while proliferating, consistent with homeostatic self-renewal, a key component of a stem cell-like functional profile.

To investigate mechanisms that may dictate the ability of PD-1^{Lo} pTfh to repopulate PD-1^{Hi} pTfh cells, we focused on the Notch signaling cascade, which has previously been implicated in regulating the developmental fate of organ-specific stem cells (37,38), memory T cells (39-41) and T follicular helper cells (42). We observed that Notch receptors 2 and 4, as well as the Notch active intracellular domain, were upregulated on CXCR5^{+} CXCR3^{+} PD-1^{Lo} cells and, to a lesser extent, on CXCR5^{+} CXCR3^{+} PD-1^{Hi} CD4 T cells from peripheral blood when compared to total CD4 T cells (Figure 6C). Moreover, inhibition of Notch signaling by gamma secretase inhibitors (GSI) in naïve T cells co-cultured with autologous naïve B cells and allogenic mDC significantly inhibited the generation of PD-1^{Hi} but not PD-1^{Lo} Tfh-like cells *in vitro* (Figure 6D). A similar inhibition in the generation of PD-1^{Hi} cells was observed when Notch signaling was blocked in sorted CXCR3^{+} PD-1^{Lo} pTfh co-cultured with autologous B cells and SEB (Figure 6E), suggesting that Notch

signaling is critical in regulating differentiation of PD-1^{Lo} CXCR5^{+} CD4 cells into PD-1^{Hi} cells. Together, these data suggest that circulating CXCR5^{+} CXCR3^{+} PD-1^{Lo} CD4 T cells represent a distinct population of progenitor cells able to repopulate the PD-1^{Hi} effector pTfh cells in a Notch-dependent fashion.

Discussion

It is highly likely that the long-lasting induction of HIV-1-specific bnAbs by vaccines will require support from Tfh or Tfh-like cells. In previous studies, peripheral $CXCR5^+$ $CXCR3^-$ $PD\text{-}1^+$ cells were found to correlate strongly with the development of HIV-1-specific bnAbs in patients with progressive diseases (16); however, such patients had continuous high-levels of HIV-1 replications and elevated levels of immune activation that hardly reflect conditions for immune induction reproducible in uninfected recipients of a prophylactic HIV-1 vaccine candidate. Here, we used HIV-1 controllers, a group of patients widely used for investigation of HIV-1 immune defense mechanisms in previous studies (43-45), as a model for studying HIV-1-specific antibodies with increased neutralizing breadth in the absence of high-levels of viremia. Our observations demonstrate that relative ratios between $CXCR5^+$ $CXCR3^+$ $PD\text{-}1^{Lo}$ and $CXCR3^+$ $CXCR5^+$ $PD\text{-}1^{Hi}$ Tfh-like cells in the blood from HIV-1 controllers correlated with increased neutralizing breadth of HIV-1 antibodies in this particular patient population. In contrast, peripheral $CXCR5^+$ $CXCR3^-$ CD4 T cells were unrelated to HIV-1-specific antibodies with broader neutralizing breadth in these patients, irrespectively of PD-1 expression. Interestingly, $CXCR5^+$ $CXCR3^+$ $PD\text{-}1^{Lo}$ Tfh-like cells expressed comparable levels of Tfh markers such as ICOS and Bcl-6 in lymphoid tissue and peripheral blood as conventional $CXCR5^+$ $CXCR3^-$ $PD\text{-}1^{Hi}$ Tfh/pTfh. Moreover, $CXCR5^+$ $CXCR3^+$ $PD\text{-}1^{Lo}$ Tfh-like cells effectively produced cytokines for stimulation of B cell development and were able to differentiate into $PD\text{-}1^{Hi}$ Tfh-like cells, although they were inferior to $CXCR3^-$ Tfh-like cells in inducing B cell Ig class switching to IgG1 in our co-culture assays. Together, these studies suggest that at least under conditions of low viral loads and immune activation, $CXCR5^+$ $CXCR3^+$ $PD\text{-}1^{Lo}$ cells may make important contributions to the induction and/or maintenance of HIV-1 antibody responses with broad neutralizing breadth.

Dendritic cells in HIV-1 controllers seem to have a distinct functional and phenotypic profile that can contribute to the induction of highly functional HIV-1-specific T cell responses. These abilities have been associated with an altered

expression profile of immunoregulatory receptors (46), and with enhanced abilities for HIV sensing and innate immune recognition (47). However, the impact of dendritic cells from these patients on Tfh development is still unclear, and investigations of dendritic cells on induction of Tfh have mostly been limited to animal studies (11,48,49) or experiments with *in vitro* generated monocyte-derived DC (MDDC) (25,33), rather than primary dendritic cells. To our knowledge, this is the first study to analyze the effects of primary dendritic cells on Tfh priming in a rare group of HIV-1 controllers who are able to generate broader neutralizing breadth in the absence of high-level viral replications. Our results demonstrate that when co-cultured with B cells, mDC from these patients have a preferential ability to induce Tfh-like cells with low expression of PD-1, and a chemokine receptor expression profile that includes co-expression of CXCR3 and CXCR5. Notably, we found that Tfh priming by mDC from controllers seems to be associated with increased transcriptional expression of genes involved in functional DC activity and in Tfh priming. Interestingly, secretion of specific cytokines, such as IL-6, a cytokine with a recognized role in Tfh priming by dendritic cells (33), tended to be higher in cultures with cells from neutralizers and was also activated in transcriptional signatures of mDC from these patients. Moreover, enhanced cell-contact dependent interactions mediated by CD40 and possibly ICOSL, which were expressed at higher levels in mDC from controller neutralizers (Figure 3E) and have previously been implicated in Tfh generation (50), may play an important role in this context. Notably, in our experimental *in vitro* system, primary mDC did not efficiently prime $CXCR3^{-}$ $CXCR5^{+}$ Tfh-like cells, suggesting that the priming of this subset is more independent of dendritic cells or might represent a different stage of T cell differentiation. Collectively, our findings highlight the importance of mDC as critical mediators of Tfh lineage commitment and suggest that manipulation of mDC might be an attractive strategy to improve Tfh differentiation in future HIV-1 vaccine studies.

Unexpectedly, this study showed that the emergence of HIV-1 antibodies with broader neutralizing breadth in HIV-1 controllers was associated with Tfh-like cells

expressing CXCR3, a surface marker denoting cells considered less efficient in supporting B cell immunoglobulin class-switching in previous *in vitro* studies (15-18). While our observations confirm that $CXCR3^+$ Tfh-like cells are inferior to $CXCR3^-$ Tfh-like cells in supporting IgG1 class switching, we did demonstrate that $CXCR3^+$ Tfh-like cells have abilities to induce class switching to IgG3 and to alternative Ig subtypes, to secrete high levels of B cell-supporting cytokines and to induce phenotypical maturation of B cells at equivalent levels as $CXCR3^-$ Tfh-like cells, at least when analyzed over a longer, six-day co-incubation period with total B cells and SEB stimulation, and not just in a short-term culture assay lasting for 48 hours (15). Together, these results suggest that $CXCR5^+$ $CXCR3^+$ Tfh-like cells can contribute to helping B cell responses, and that $CXCR5^+$ $CXCR3^-$ and $CXCR5^+$ $CXCR3^+$ pTfh might have distinct, but partially overlapping roles for supporting B cells. Consistent with a role as circulating memory cells, $CXCR5^+$ $CXCR3^+$ $PD\text{-}1^{Lo}$cells in HIV-1 controllers may primarily contribute to maintaining long-term survival of B cells producing more broadly cross-reactive antibodies, and not to the initial priming of such immune responses, which is likely to preferentially occur in lymph node germinal centers and may largely be independent of circulating Tfh-like cells. A preferential role of $CXCR3^+$ Tfh-like cells in maintaining or expanding pre-existing B cell responses, but not in the initial priming of new antigen-specific B cells, was also hypothesized in alternative contexts associated with limited antigen exposure, such as in recipients of vaccines against Influenza (19). In contrast, in HIV-1 progressors with continuously-ongoing high-level viremia, maintenance of HIV-1-specific B cells may more significantly depend on the presence of elevated amounts of circulating viral antigens. Notably, our data do not exclude the possibility that $CXCR3^-$ pTfh, which were also significantly elevated in controller neutralizers (Figure 1B), participate individually or in collaboration with $CXCR3^+$ pTfh in generating or maintaining more broadly-neutralizing antibody-secreting B cells in these patients.

A large number of studies suggest that circulating $CXCR5^+$ T cells are memory Tfh cells (3), but the dynamics of their development and long-term survival remain

poorly understood. Our data suggest that phenotypically-defined subsets of circulating CXCR5^{+} CD4 T cells may not only differ by effector functions, but also involve a developmental and maturational aspect. A linear developmental hierarchy from long-lasting immature central-memory and stem cell-memory to short-lived effector-memory cells is experimentally well validated within the CD8 T cell memory compartment (36), and has also been suggested to occur with CD4 T cells (51). The results presented here suggest that a similar developmental hierarchy also exists within the pools of circulating Tfh-like cells, and that PD-1^{Lo} Tfh represent a long-lived precursor cell population that can replenish the more mature and short-lived PD-1^{Hi} effector Tfh cells. Interestingly, these PD-1^{Lo} Tfh-like cells included a substantial proportion of CD45RO^{-} naive-like T cells, a cell population that was excluded in prior studies (15-17), but includes a fraction of highly-immature memory T cells with increased stem cell-like properties (36). The ability to maintain a larger proportion of PD-1^{Lo} memory Tfh-like cells that are enriched for a T memory stem cell phenotype relative to PD-1^{Hi} pTfh could represent a distinct aspect of HIV-1 controllers with more broadly neutralizing antibody responses, and appears to separate these patients from HIV-1 progressors in which high-level viremia may lead to more differentiated and possibly more exhausted PD-1^{Hi} pTfh cell populations (52). Notably, an optimal balance between immature precursor cells and more committed effector cells has previously also been found to be critical for regulating CD8 T cell immunity (53). In addition, a higher proportion of total immature memory CD8 and CD4 T cells are associated with improved prognosis in chronic HIV-1 infection (54) and can be enriched in the absence of viremia and immune activation in treated HIV-1-positive individuals (55). Interestingly, we found evidence that Notch signaling, previously mostly shown to regulate hematopoietic and thymic precursor cell differentiation (37,38), is also involved in regulating the transition of long-lasting PD-1^{Lo} into short-lived PD-1^{Hi} Tfh-like cells. This suggest that stem cell pathways, previously recognized in the context of traditional organ-specific stem cells, may also contribute to regulation and fate decisions within the memory Tfh pools, and may offer molecular targets for

selectively influencing memory Tfh development. A role for Notch in Tfh memory evolution is also consistent with the recent observation that Notch signaling was necessary for Tfh differentiation in experimental animal models (42).

Taken together, these studies demonstrate that the CXCR5^{+} CXCR3^{+} PD-1^{Lo} Tfh-like population serves as precursor cells for PD-1^{Hi} cells, supports B cell development through cytokine secretion, is associated with maintenance of more broadly-neutralizing HIV-1 antibody responses in the absence of high-level HIV-1 viremia and can be selectively primed by dendritic cells from HIV-1 controllers with neutralizing antibody responses. These studies may help to delineate mechanisms for inducing HIV-1 antibodies with higher levels of neutralizing breadth by prophylactic vaccines.

Methods

Study Participants

HIV-1 controllers who had maintained < 1500 copies/ml HIV-1 viral loads (VL) for a median of 5 years (range 2-14) in the absence of antiretroviral therapy, with (neutralizers, NT, n=25, median VL 123 copies/ml, range 20-1400 copies/ml; median CD4 counts 769.5 cells/ml, range 418-1545 cells/ml) or without (non-neutralizers, NN, n=20; median VL 75 copies/ml, range 48-1470 copies/ml; median CD4 counts 844.5 cells/ml, range 407-2117 cells/ml) neutralizing antibodies against Tier-2/3 HIV-1 viruses, untreated chronic progressors (CP, n=14, median VL 28352.5 copies/ml, range 2368-90500 copies/ml; median CD4 T cell counts 313 cells/ml, range 88-955 cells/ml), ART-treated chronically HIV-1-infected patients with suppressed HIV-1 viremia (H, n=14, median VL <49 copies/ml; median CD4 T cell counts 490 cells/ml, range 183-964 cells/ml) and HIV-1 seronegative healthy persons (NG, n=14) were recruited for this study. Samples of mononuclear cells extracted from inguinal lymph nodes were obtained by surgical excision from HIV-1 negative study persons. Mononuclear samples from human tonsil tissue of HIV-1 negative individuals who underwent routine tonsillectomies were obtained as previously described (52).

Analysis of the neutralizing breadth of HIV-1-specific antibodies

As previously described (56), HIV-1 neutralization breadth was measured in a TZM-bl cell-based pseudovirus neutralization assay against a panel of Env-pseudoviruses derived from 9 Clade B Tier 2 and two Tier 3 neutralization sensitivities: AC10.0.29*, RHPA4259.7*, THRO4156.18*, REJO4541.67*, WITO4160.33*, TRO.11*, SC422661.8*,QH0692.42*, CAAN5342.A2# and Tier 3: PVO.4* and TRJO4551.58*. The Clade B and C isolates are denoted by the superscripts * and # respectively. Neutralization was defined as at least 50% inhibition of infection at a 1:20 dilution. The neutralization breadth was defined as the percentage of the 11 isolates neutralized by each plasma sample. All samples were screened for non-HIV-1-specific neutralization using murine leukemia virus-pseudotyped virions

Cell isolation

Total $CD19^-$ $BDCA1^+$ and $BDCA3^+$ myeloid dendritic cells (mDC) were purified from total PBMC or lymph node suspensions by immunomagnetic enrichment as previously described (47) (purity > 90%). Naïve $CD4^+$ T cells and naïve $CD27^-$ B cells were isolated using immunomagnetic negative selection kits (Miltenyi Biotec, Naïve CD4+ T cell Isolation Kit II and Naïve B cell Isolation Kit II human), leading to cell purity of >95%. MS and LD columns and/or the AutoMACS (Miltenyi Biotec) system were used for cell isolation.

In vitro DC-based priming of Tfh-like cells

$5x10^4$ freshly isolated naïve CD4 T cells were co-cultured with $5x10^4$ autologous naïve B cells in the presence or absence of $5x10^4$ allogeneic mDC from different patient cohorts in 96 round-bottom well plates for 7 days. Naïve T and B cells were obtained from the same donors, but different individuals were used for each experiment. Presence of $CXCR5^+$ $PD\text{-}1^+$ Tfh-like cells was analyzed by flow cytometry at the end of the culture. Naïve B cells and T cells cultured alone with media only were used as negative controls. At day 7 of culture, supernatants were collected for cytokine and antibody quantification, and cells were harvested to analyze the phenotype of cultured T and B cells. When indicated, cells were cultured in the presence of 5μg/ml anti-human CD40 neutralizing mAb (Clone 82102, R&D Systems) or an Isotypic control mAb (Invitrogen). In some experiments, T-B-mDC co-cultures were conducted in the presence of either 100nM gamma secretase inhibitors (GSI; MK-0752; SelleckChem) or DMSO as a control. *In-vitro* generation of Tfh-like cells under contact-dependent and independent conditions was evaluated by co-culturing naïve B cells and T cells as previously described in the lower chamber of 96-well trans-well plates (Corning) directly in contact with mDC or with mDC plated on the upper trans-well chamber for 7 days.

Functional assays with ex-vivo isolated human pTfh populations

Human $CXCR3^+$ and $CXCR3^-$ $PD\text{-}1^{Lo}$ and $PD\text{-}1^{Hi}$ $CXCR5^+$ CD4 T cells (pTfh) were sorted in parallel with total $CD3^-CD19^+$ B cells in PBMC from healthy donors and cultured in the presence of 2μg/ml of Staphylococcal endotoxin B (SEB) for 6 days.

At day 6 of culture, supernatants were collected for cytokine and antibody quantification, and cells were harvested to analyze phenotype of cultured pTfh and B cells. In some experiments, pTfh were labeled with 5μM of Carboxyfluorescein succinimidyl ester (CFSE, Life Technologies) to track cell proliferation in the indicated conditions.

Luminex analysis

Concentrations of human cytokines (IL-6, IL-10, IL-21, IL-12p70, IL-22, TNFα, GM-CSF) and immunoglobulins (IgM, IgA, IgG) were analyzed in culture supernatants using Human Th17 magnetic bead and Human Immunoglobulin magnetic Luminex kits (Millipore), respectively, following the manufacturer's instructions.

Gene expression analysis by RNA-Seq

Total RNA was obtained from sorted $CD14^{-}$ $CD11c^{Hi}$ $HLADR^{+}$ mDC from peripheral blood of controllers neutralizers (n=4) and controllers non-neutralizers (n=4). Subsequently, total RNA was extracted using a commercial kit recommended for low numbers of cells (*mir*Vana™ Isolation Kit; Life Technologies™). RNA-Seq libraries from mDC from each patient group were generated as previously described (57). Briefly, whole transcriptome amplification (WTA) and tagmentation-based library preparation was performed using SMART-seq2 (57), followed by sequencing on a NextSeq 500 Instrument (Illumina). FASTQ files were obtained using the Illumina demultiplexing pipeline. STAR (58) and RSEM (59) was used to align to HG38 and to calculate the raw counts for genes, respectively. TPM values were then normalized among all samples using the upper quantile normalization method. Subsequently, genes differentially expressed between mDC from controller neutralizers and non-neutralizers were identified by DESeq2 (30). Ingenuity Pathway Analysis (IPA) was used to functionally categorize differentially expressed genes, and to biocomputationally identify putative upstream regulators responsible for differential gene expression signatures. The original RNAseq data is available at NCBI GEO public database with accession number GSE90897.

Flow cytometry

Ex vivo and cultured PBMC, as well as tonsil and lymph node cell extracts were stained with LIVE/DEAD cell blue viability dye (Invitrogen, Carlsbad, CA) and different panels of monoclonal antibodies. For Tfh/pTfh identification or characterization, the following mAbs were used: anti-human CD4 (RPA-T4, BD), CD3 (OKT3), CXCR5 (J252D4), CXCR3 (G025H7), PD-1 (H12.2H7), ICOS (C.398.4A) (Biolegend). For phenotypical analysis of cultured B cells, anti-CD19, CD38 (Biolegend), CD27 (M-T271, BD) mAbs were included in the panel. In addition, mDC from different study cohorts were characterized using anti-human PD-L1 (29E-2A3), CD40 (5C3), CD86 (IT 2.2), HLA-DR (L243), CD11c (3.9), ICOS-L (2D3) (Biolegend), and CD14 (MØP9, BD). mDC were identified from bulk PBMCs as a population of viable $CD14^-$ lymphocytes expressing high levels of CD11c and HLA-DR. For intracellular staining, cells were treated with a commercial fixation/permeabilization kit (BioLegend) according to the manufacturer's protocol and incubated with anti-human Bcl-6 (K112-91, BD) and Tbet (4B10, BioLengend) mAbs. Subsequently, samples were analyzed on a Fortessa cytometer (BD Biosciences, San Jose, CA). Data were analyzed with FlowJo software (Tree Star).

Statistics analysis

Significance of phenotypic differences between the different patient cohorts were assessed using Mann Whitney U tests for individual comparisons or Kruskal-Wallis test followed by Dunn's test for multiple comparisons. To calculate significance of differences observed within the same individuals or experiments with different treatments, a Wilcoxon matched-pairs signed-rank test or a Friedman test followed by a Dunn's tests were used for individual or multiple comparisons, respectively. To analyze statistically significant differences in HLA-I and HLA-II allele distribution between controller neutralizers and non-neutralizers, a chi-square test was used and p-values were adjusted by the Bonferroni correction. To investigate transcriptional expression patterns in mDC from neutralizers and non-neutralizers by RNAseq, DESeq2 (30) was used to access the differentially expressed genes after using STAR [https://www.ncbi.nlm.nih.gov/pubmed/23104886] and RSEM [https://www.ncbi.nlm.nih.gov/pubmed/21816040] for the alignment to HG38.

Data were visualized as heatmaps, with unsupervised hierarchical clustering analysis using the Ward method. In addition, the significant canonical pathways and upstream regulators were predicted by Ingenuity Pathway Analysis using Fisher's exact test.

Study approval

All subjects gave written informed consent and the study was approved by the Institutional Review Board of Massachusetts General Hospital/Partners Healthcare. Individuals undergoing lymph node biopsy procedure were recruited at the University of Hamburg (Germany) and at Massachusetts General Hospital in Boston, according to protocols approved by the local Ethics Committee. Human tonsil samples were obtained at Martin Memorial Hospital, Florida, following a locally-approved IRB protocol.

Author contributions

X.G.Y., E.M.G. and M.Lic. developed the research idea and study concept, designed the study and wrote the manuscript;

X.G.Y. supervised the study;

E.M.G. designed and conducted most experiments;

J.C. and T.H. provided technical help in most experiments;

Z.O. supervised statistical analysis and provided bioinformatic support for RNA-Seq data analyses;

M. Lin. and D.E.K. provided some phenotyping data on lymph node samples from HIV-1 negative donors;

A.K.S. and K.E.K performed the RNAseq experiments;

B.D.W. provided PBMC samples from HIV-1 infected patients;

J.S.Z.W., J.V.L, M.Lin., F.P. and D.E.K provided human lymph node samples;

R.C. and E.K.H. provided human tonsil samples;

B.D.W., R.C., A.K.S., D.E.K., E.K.H. participated in study-related discussions and critically reviewed the manuscript.

Acknowledgments

This work was supported for the US National Institutes of Health (grants AI078799, AI089339, HL121890, AI098484, HL126554, AI116228 and AI087452 to XGY; AI098487 and AI106468 to ML). PBMC sample collection was supported by the Bill and Melinda Gates Foundation (OPP 1066973), the Mark and Lisa Swartz Foundation, the Ragon Institute of MGH, MIT and Harvard, and the International HIV Controller Consortium. AKS was supported by the Searle Scholars Foundation, the Beckman Young Investigator Program, and a NIH New Innovator Award (DP2 OD020839). DEK is supported by a Research Scholar Career Award of the Quebec Health Research Fund (FRQS). Lymph node sample collection was supported by NIH Scripps Center for HIV/AIDS Vaccine and Immunogen Discovery (CHAVI-ID, 1UM1-AI100663 to BDW and DEK; tonsil sample collection was supported by NIH grant AI106482 to EKH.

References

1. Kwong PD, Mascola JR. Human antibodies that neutralize HIV-1: identification, structures, and B cell ontogenies. *Immunity.* Sep 21 2012;37(3):412-425.

2. Burton DR, Mascola JR. Antibody responses to envelope glycoproteins in HIV-1 infection. *Nature immunology.* Jun 2015;16(6):571-576.

3. Crotty S. T follicular helper cell differentiation, function, and roles in disease. *Immunity.* Oct 16 2014;41(4):529-542.

4. Craft JE. Follicular helper T cells in immunity and systemic autoimmunity. *Nature reviews. Rheumatology.* Jun 2012;8(6):337-347.

5. Nurieva RI, Chung Y, Martinez GJ, et al. Bcl6 mediates the development of T follicular helper cells. *Science.* Aug 21 2009;325(5943):1001-1005.

6. Crotty S. Follicular helper CD4 T cells (TFH). *Annual review of immunology.* 2011;29:621-663.

7. Avery DT, Bryant VL, Ma CS, de Waal Malefyt R, Tangye SG. IL-21-induced isotype switching to IgG and IgA by human naive B cells is differentially regulated by IL-4. *Journal of immunology.* Aug 1 2008;181(3):1767-1779.

8. Bentebibel SE, Schmitt N, Banchereau J, Ueno H. Human tonsil B-cell lymphoma 6 (BCL6)-expressing CD4+ T-cell subset specialized for B-cell help outside germinal centers. *Proceedings of the National Academy of Sciences of the United States of America.* Aug 16 2011;108(33):E488-497.

9. Vinuesa CG, Linterman MA, Goodnow CC, Randall KL. T cells and follicular dendritic cells in germinal center B-cell formation and selection. *Immunological reviews.* Sep 2010;237(1):72-89.

10. Liu D, Xu H, Shih C, et al. T-B-cell entanglement and ICOSL-driven feed-forward regulation of germinal centre reaction. *Nature.* Jan 8 2015;517(7533):214-218.

11. Goenka R, Barnett LG, Silver JS, et al. Cutting edge: dendritic cell-restricted antigen presentation initiates the follicular helper T cell program but cannot complete ultimate effector differentiation. *Journal of immunology.* Aug 1 2011;187(3):1091-1095.

12. Yao C, Zurawski SM, Jarrett ES, et al. Skin dendritic cells induce follicular helper T cells and protective humoral immune responses. *The Journal of allergy and clinical immunology.* May 9 2015.

13. Ise W, Inoue T, McLachlan JB, et al. Memory B cells contribute to rapid Bcl6 expression by memory follicular helper T cells. *Proceedings of the National Academy of Sciences of the United States of America.* Aug 12 2014;111(32):11792-11797.

14. Breitfeld D, Ohl L, Kremmer E, et al. Follicular B helper T cells express CXC chemokine receptor 5, localize to B cell follicles, and support immunoglobulin production. *The Journal of experimental medicine.* Dec 4 2000;192(11):1545-1552.

15. Morita R, Schmitt N, Bentebibel SE, et al. Human blood CXCR5(+)CD4(+) T cells are counterparts of T follicular cells and contain specific subsets that

differentially support antibody secretion. *Immunity.* Jan 28 2011;34(1):108-121.

16. Locci M, Havenar-Daughton C, Landais E, et al. Human circulating PD-1+CXCR3-CXCR5+ memory Tfh cells are highly functional and correlate with broadly neutralizing HIV antibody responses. *Immunity.* Oct 17 2013;39(4):758-769.

17. Cubas R, van Grevenynghe J, Wills S, et al. Reversible Reprogramming of Circulating Memory T Follicular Helper Cell Function during Chronic HIV Infection. *Journal of immunology.* Nov 6 2015.

18. Schmitt N, Bentebibel SE, Ueno H. Phenotype and functions of memory Tfh cells in human blood. *Trends in immunology.* Sep 2014;35(9):436-442.

19. Bentebibel SE, Lopez S, Obermoser G, et al. Induction of ICOS+CXCR3+CXCR5+ TH cells correlates with antibody responses to influenza vaccination. *Science translational medicine.* Mar 13 2013;5(176):176ra132.

20. Matsui K, Adelsberger JW, Kemp TJ, Baseler MW, Ledgerwood JE, Pinto LA. Circulating CXCR5+CD4+ T Follicular-Like Helper Cell and Memory B Cell Responses to Human Papillomavirus Vaccines. *PloS one.* 2015;10(9):e0137195.

21. Iyer SS, Gangadhara S, Victor B, et al. Codelivery of Envelope Protein in Alum with MVA Vaccine Induces CXCR3-Biased CXCR5+ and CXCR5- CD4 T Cell Responses in Rhesus Macaques. *Journal of immunology.* Aug 1 2015;195(3):994-1005.

22. Velu V, Mylvaganam GH, Gangadhara S, et al. Induction of Th1-Biased T Follicular Helper (Tfh) Cells in Lymphoid Tissues during Chronic Simian Immunodeficiency Virus Infection Defines Functionally Distinct Germinal Center Tfh Cells. *Journal of immunology.* Sep 1 2016;197(5):1832-1842.

23. Walker BD, Yu XG. Unravelling the mechanisms of durable control of HIV-1. *Nature reviews. Immunology.* Jul 2013;13(7):487-498.

24. Doria-Rose NA, Klein RM, Daniels MG, et al. Breadth of human immunodeficiency virus-specific neutralizing activity in sera: clustering analysis and association with clinical variables. *Journal of virology.* Feb 2010;84(3):1631-1636.

25. Schmitt N, Morita R, Bourdery L, et al. Human dendritic cells induce the differentiation of interleukin-21-producing T follicular helper-like cells through interleukin-12. *Immunity.* Jul 17 2009;31(1):158-169.

26. Yu D, Rao S, Tsai LM, et al. The transcriptional repressor Bcl-6 directs T follicular helper cell lineage commitment. *Immunity.* Sep 18 2009;31(3):457-468.

27. Rasheed AU, Rahn HP, Sallusto F, Lipp M, Muller G. Follicular B helper T cell activity is confined to CXCR5(hi)ICOS(hi) CD4 T cells and is independent of CD57 expression. *European journal of immunology.* Jul 2006;36(7):1892-1903.

28. Sage PT, Sharpe AH. T follicular regulatory cells in the regulation of B cell responses. *Trends in immunology.* Jul 2015;36(7):410-418.

29. Mullen AC, High FA, Hutchins AS, et al. Role of T-bet in commitment of TH1 cells before IL-12-dependent selection. *Science.* Jun 8 2001;292(5523):1907-1910.
30. Love MI, Huber W, Anders S. Moderated estimation of fold change and dispersion for RNA-seq data with DESeq2. *Genome biology.* 2014;15(12):550.
31. Choi YS, Kageyama R, Eto D, et al. ICOS receptor instructs T follicular helper cell versus effector cell differentiation via induction of the transcriptional repressor Bcl6. *Immunity.* Jun 24 2011;34(6):932-946.
32. Nish SA, Schenten D, Wunderlich FT, et al. T cell-intrinsic role of IL-6 signaling in primary and memory responses. *eLife.* May 19 2014;3:e01949.
33. Chakarov S, Fazilleau N. Monocyte-derived dendritic cells promote T follicular helper cell differentiation. *EMBO molecular medicine.* May 01 2014;6(5):590-603.
34. Yamasaki S, Shimizu K, Kometani K, Sakurai M, Kawamura M, Fujii SI. In vivo dendritic cell targeting cellular vaccine induces CD4+ Tfh cell-dependent antibody against influenza virus. *Scientific reports.* Oct 14 2016;6:35173.
35. Deenick EK, Chan A, Ma CS, et al. Follicular helper T cell differentiation requires continuous antigen presentation that is independent of unique B cell signaling. *Immunity.* Aug 27 2010;33(2):241-253.
36. Gattinoni L, Lugli E, Ji Y, et al. A human memory T cell subset with stem cell-like properties. *Nature medicine.* Oct 2011;17(10):1290-1297.
37. Artavanis-Tsakonas S, Rand MD, Lake RJ. Notch signaling: cell fate control and signal integration in development. *Science.* Apr 30 1999;284(5415):770-776.
38. Kojika S, Griffin JD. Notch receptors and hematopoiesis. *Experimental hematology.* Sep 2001;29(9):1041-1052.
39. Maekawa Y, Ishifune C, Tsukumo S, Hozumi K, Yagita H, Yasutomo K. Notch controls the survival of memory CD4+ T cells by regulating glucose uptake. *Nature medicine.* Jan 2015;21(1):55-61.
40. Mota C, Nunes-Silva V, Pires AR, et al. Delta-like 1-mediated Notch signaling enhances the in vitro conversion of human memory CD4 T cells into FOXP3-expressing regulatory T cells. *Journal of immunology.* Dec 15 2014;193(12):5854-5862.
41. Tsukumo S, Yasutomo K. Notch governing mature T cell differentiation. *Journal of immunology.* Dec 15 2004;173(12):7109-7113.
42. Auderset F, Schuster S, Fasnacht N, et al. Notch signaling regulates follicular helper T cell differentiation. *Journal of immunology.* Sep 1 2013;191(5):2344-2350.
43. Chen H, Li C, Huang J, et al. CD4+ T cells from elite controllers resist HIV-1 infection by selective upregulation of p21. *The Journal of clinical investigation.* Apr 2011;121(4):1549-1560.
44. Migueles SA, Laborico AC, Shupert WL, et al. HIV-specific CD8+ T cell proliferation is coupled to perforin expression and is maintained in nonprogressors. *Nature immunology.* Nov 2002;3(11):1061-1068.

45. Saez-Cirion A, Pancino G. HIV controllers: a genetically determined or inducible phenotype? *Immunological reviews.* Jul 2013;254(1):281-294.
46. Huang J, Burke PS, Cung TD, et al. Leukocyte immunoglobulin-like receptors maintain unique antigen-presenting properties of circulating myeloid dendritic cells in HIV-1-infected elite controllers. *Journal of virology.* Sep 2010;84(18):9463-9471.
47. Martin-Gayo E, Buzon MJ, Ouyang Z, et al. Potent Cell-Intrinsic Immune Responses in Dendritic Cells Facilitate HIV-1-Specific T Cell Immunity in HIV-1 Elite Controllers. *PLoS pathogens.* Jun 2015;11(6):e1004930.
48. Ballesteros-Tato A, Randall TD. Priming of T follicular helper cells by dendritic cells. *Immunology and cell biology.* Jan 2014;92(1):22-27.
49. Baumjohann D, Okada T, Ansel KM. Cutting Edge: Distinct waves of BCL6 expression during T follicular helper cell development. *Journal of immunology.* Sep 1 2011;187(5):2089-2092.
50. Ma DY, Clark EA. The role of CD40 and CD154/CD40L in dendritic cells. *Seminars in immunology.* Oct 2009;21(5):265-272.
51. Muranski P, Borman ZA, Kerkar SP, et al. Th17 cells are long lived and retain a stem cell-like molecular signature. *Immunity.* Dec 23 2011;35(6):972-985.
52. Cubas RA, Mudd JC, Savoye AL, et al. Inadequate T follicular cell help impairs B cell immunity during HIV infection. *Nature medicine.* Apr 2013;19(4):494-499.
53. Paley MA, Kroy DC, Odorizzi PM, et al. Progenitor and terminal subsets of CD8+ T cells cooperate to contain chronic viral infection. *Science.* Nov 30 2012;338(6111):1220-1225.
54. Ribeiro SP, Milush JM, Cunha-Neto E, et al. The CD8(+) memory stem T cell (T(SCM)) subset is associated with improved prognosis in chronic HIV-1 infection. *Journal of virology.* Dec 2014;88(23):13836-13844.
55. Vigano S, Negron J, Ouyang Z, et al. Prolonged Antiretroviral Therapy Preserves HIV-1-Specific CD8 T Cells with Stem Cell-Like Properties. *Journal of virology.* Aug 1 2015;89(15):7829-7840.
56. Seaman MS, Janes H, Hawkins N, et al. Tiered categorization of a diverse panel of HIV-1 Env pseudoviruses for assessment of neutralizing antibodies. *Journal of virology.* Feb 2010;84(3):1439-1452.
57. Trombetta JJ, Gennert D, Lu D, Satija R, Shalek AK, Regev A. Preparation of Single-Cell RNA-Seq Libraries for Next Generation Sequencing. *Current protocols in molecular biology / edited by Frederick M. Ausubel ... [et al.].* 2014;107:4 22 21-24 22 17.
58. Dobin A, Davis CA, Schlesinger F, et al. STAR: ultrafast universal RNA-seq aligner. *Bioinformatics (Oxford, England).* Jan 1 2013;29(1):15-21.
59. Li B, Dewey CN. RSEM: accurate transcript quantification from RNA-Seq data with or without a reference genome. *BMC bioinformatics.* 2011;12:323.

Figure legends

Figure 1. CXCR5$^+$ CXCR3$^+$ PD-1^{Lo} Tfh-like cells are enriched in controller neutralizers and associated with neutralizing breadth against HIV-1. (A): Proportions of total CXCR3$^+$ PD-1$^+$ CXCR5$^+$ or CXCR3$^-$ PD-1$^+$ CXCR5$^+$ subpopulations within total CD4 T cells in the blood from HIV-1-infected controller non-neutralizers (NN, n=20) and neutralizers (NT, n=25). Statistical differences were calculated using a Wilcoxon matched-pairs test in each group of patients (**p<0.01). (B): Proportions of PD-1^{Lo} or PD-1^{Hi} cells within CXCR3$^+$ CXCR5$^+$ and CXCR3$^-$ CXCR5$^+$ CD4 T cell populations from indicated study cohorts. Statistical differences between NN and NT were calculated separately for each individual pTfh subset using a Mann Whitney U test (* p<0.05). (C): Spearman correlations between ratios of PD-1^{Lo} vs PD-1^{Hi} cells within CXCR3$^+$ (left) and CXCR3$^-$ (right) CXCR5$^+$ CD4 T cells from controller neutralizers and the corresponding breadth of HIV-1-specific neutralizing antibodies. Numbers included on the top right corner of each plot reflect nominal P-values and spearman R values.

Figure 2. Primary mDCs from controller neutralizers efficiently induce Tfh-like cells *in vitro*. (A): Flow cytometry analysis of CXCR5 and PD-1 expression on naive CD4 T cells from an HIV-1 negative donor cultured for 7 days in the presence of media alone (left) or autologous naïve B cells in the absence (middle) or the presence (right) of allogeneic mDCs isolated from an additional HIV-1 negative donor. Rectangles highlight CXCR5$^+$ CD4 T cells expressing either low or high levels of PD-1 (PD-1^{Lo} and PD-1^{Hi}, respectively). Dot plots from a representative experiment are shown. (B): Intracellular Bcl-6 expression in indicated CD4 T cell subsets after co-culture with mDCs for 7 days. Left panel shows dot plots from one representative experiment. Right panel shows cumulative mean fluorescence intensity of Bcl-6 data from n=15 HIV-1 negative study subjects. Statistical significance was calculated using a Friedman test followed by Dunn's test (**p< 0.01; ***p<0.001). (C): Proportions of PD-1^{Hi} (left) and PD-1^{Lo} (right) CXCR5$^+$ CD4 T cells differentiated from naïve CD4 T cells after 7 days of culture in the presence of autologous naïve B cells (violet) alone or in combination with allogeneic mDCs from HIV-1 negative donors (NG; blue, n=16), controller non-neutralizers (NN; dark green n=16), neutralizers (NT; light green n=20), untreated (CP; orange n=14) and HAART-treated (H; purple n=14) chronic progressors. Statistical significance between DC from neutralizers and other conditions was calculated using a Kruskal-Wallis test followed by a Dunn's test (*p<0.05; ***p<0.001). (D): Ratios of PD-1^{Lo} vs PD-1^{Hi} CXCR5$^+$ CD4 T cells differentiated in the presence of allogeneic mDCs from different study cohorts. Statistical significance between mDCs from NT vs other conditions was calculated using a Kruskal-Wallis test followed by a Dunn's test (**p<0.01).

Figure 3. Transcriptional analysis of dendritic cells from HIV-1 controller neutralizers. (A): Heatmap representing 930 genes differentially expressed (FDR-adjusted p<0.05) between peripheral blood mDCs from Neutralizers (NT) and Non Neutralizers (NN) (n=4 patients in each group). (B): Left panel: Canonical pathways

significantly upregulated (red) and downregulated (blue) (Fisher's exact test, – Log10 p values for each represented pathways are shown) in transcriptional signatures in mDC from NT, as predicted by Ingenuity Pathway Analysis (IPA). Pathways in grey are significant but without known degree of functional activation/inhibition. Right Panel: Circos plot representing genes shared between pathways differentially expressed in mDC from NT. Inner circle reflects the Log2 Fold change in gene expression intensity between NT vs NN. Pathways predicted to be activated in NT are highlighted in red in outer circle; pathways in grey are significant but with unknown degree of functional activation. (C): Significant putative upstream regulators with predicted activating (red) or inhibitory (blue) influence on transcriptional signatures in mDC from NT, as determined by IPA. (D): Predicted network interactions of 5 putative upstream regulators of transcriptional signatures in mDC from NT. Activating impulses are highlighted in orange, inhibitory signals are marked in blue. Target genes upregulated in mDC from NT are labeled in red, downregulated genes are labeled in green. (E): Mean Fluorescence Intensity of surface levels of ICOS ligand (ICOS-L) and CD40 assessed by flow cytometry in gated mDCs from HIV-1 controller non-neutralizers (NN; dark green, n=18) and neutralizers (NT; light green n=24). Statistical significance was calculated using a two-tailed Mann-Whitney U test (*p<0.05). (F): Changes in proportions of PD-1^{Lo} (left) and PD-1^{Hi} (right) Tfh-like cells generated in the presence or the absence of anti-CD40 blocking antibodies (n=6 experiments). Differences were tested for significance using a two-tailed Wilcoxon matched-pairs signed rank test (*p<0.05).

Figure 4. CXCR3^{+} PD-1^{Lo} pTfh cells support B cell activation and differentiation. (A): Dot plots reflect CXCR5 vs PD-1 expression on sorted CXCR3^{+} and CXCR3^{-} PD-1^{Lo} and PD-1^{Hi} pTfh cells on day 6 in co-culture with autologous total B cells in the presence of SEB in a representative experiment. Numbers above the gates represent percentages of cells. (B-C): Proportions of PD-1^{Hi} (B) and PD-1^{Lo} (C) CD4 T cells after six-day culture of isolated CXCR3^{+} PD-1^{Lo} (n=5), CXCR3^{+} PD-1^{Hi} (n=5), CXCR3^{-} PD-1^{Lo} (n=4) and CXCR3^{-} PD-1^{Hi} (n=5) cells with autologous B cells and SEB. (D): Representative flow cytometry analysis showing CD38 vs CD27 surface expression on gated CD19^{+} B cells on day 6 of co-culture with SEB alone or the indicated pTfh populations. Numbers within the gates represent percentages of cells. (E): Proportions of CD38^{Int} CD27^{Int} activated memory and CD38^{Hi} CD27^{Hi} plasmablast (PB)-like B cells on day 6 of co-culture with indicated pTfh populations. CXCR3^{+} PD-1^{Lo} (n=5), CXCR3^{+} PD-1^{Hi} (n=5), CXCR3^{-} PD-1^{Lo} (n=4) and CXCR3^{-} PD-1^{Hi}. (n=5). Differences between each condition with indicated pTfh subset and control B cells activated with SEB alone were tested for statistical significance using a Kruskal-Wallis test followed by Dunn's test (*p<0.05). (F-G): Luminex analysis of indicated cytokine (F) and Ig (G) concentrations present in supernatants on day 6 in the indicated co-cultures with CXCR3^{+} PD-1^{Lo} (n=5) CXCR3^{+} PD-1^{Hi} (n=5), CXCR3^{-} PD-1^{Lo} (n=4) and CXCR3^{-} PD-1^{Hi} (n=5) pTfh. Statistical significance was calculated using a Kruskal-Wallis test followed by a Dunn's test (**p<0.01).

Figure 5. Characterization of memory cell subsets within Tfh-like cells. (A-B): Representative flow cytometry analysis of memory cell subsets in total CD4 T cells (A) and in PD-1^{Lo} and PD-1^{Hi} CXCR5^{+} CXCR3^{+} and CXCR5^{+} CXCR3^{-} pTfh cells (B). CCR7 vs CD45RO expression define central memory (CM), effector memory (EM), terminally differentiated (TD) and naïve-like (NA-like) T cells (upper panels). NA-like T cells are subdivided into memory stem cells (SCM) and naïve (NA) cells based on expression levels of CD95 (lower panels). (C-D) Proportions of memory subsets within PD-1^{Lo} and PD-1^{Hi} CXCR3^{+} and CXCR3^{-} cells, and total CD4 T cells (CD4) from peripheral blood (P. Blood; upper panel, n=7), tonsils (middle panel, n=8) and lymph nodes (lower panel, n=7) (C). Proportions of T memory stem cells (SCM) within each pTfh subset from the indicated compartments are represented separately in (D). Statistical significance within individual subset (C) and in T_{SCM} proportions across different subsets (D) was calculated using a Friedman test followed by a Dunn's test (*p<0.05; **p<0.01; ***p<0.001).

Figure 6. CXCR3^{+} PD-1^{Lo} pTfh cells can differentiate into PD-1^{Hi} cells in a Notch-dependent fashion. (A): Sorted CXCR5^{+} CXCR3^{+} PD-1^{Lo} Tfh-like cells were cultured with autologous B cells and SEB for 6 days (left plot). PD-1^{Lo} and PD-1^{Hi} events from these cultures were selectively resorted and co-cultured for 6 additional days with B cells and SEB. Right plots reflect PD-1 expression on resorted PD-1^{Lo} and PD-1^{Hi} cells after the second six-day culture assay. Dot plots from a representative experiment are shown. Numbers on the gates represent the proportion of cells. (B): Proportions of remaining PD-1^{Lo} and PD-1^{Hi} cells detected on day six of co-culture of freshly-sorted (F) or resorted (R) CXCR5^{+} CXCR3^{+} PD-1^{Lo} (n=5), CXCR5^{+} CXCR3^{+} PD-1^{Hi} (n=5) and CXCR5^{+} CXCR3^{-} PD-1^{Hi} (n=5) pTfh with total B cells and SEB. Statistical significance was calculated using a Friedman test followed by Dunn's test (*p<0.05; **p<0.01). (C): Mean fluorescence intensity of Notch 1, 2, 4 and Intracellular Notch (ICN) in pTfh subsets and total CD4 T cells (n=8). Statistical significance was calculated using a Friedman test followed by a Dunn's test (*p<0.05; **p<0.01, *** p<0.01). (D): Proportions of PD-1^{Lo} or PD-1^{Hi} Tfh-like cells generated upon co-culture of naive CD4 T cells with autologous B cells and allogeneic mDCs in the presence of gamma secretase inhibitors (GSI) in comparison to 100nM DMSO (n=6). Statistical significance was calculated using a two-tailed Wilcoxon matched-pairs signed-rank test (*p<0.05). (E): Proportions of PD-1^{Hi} T cells derived from CXCR5^{+} CXCR3^{+} PD-1^{Lo} CD4 T cells after 6 days of co-culture with autologous B cells and SEB in the presence of GSI compared to DMSO (n=6). Statistical significance was calculated using a two-tailed Wilcoxon matched-pairs signed-rank test (*p<0.05).

Supplemental Figure Legends

Supplemental Figure 1. CXCR3 and PD-1 expression defines Tfh-like subsets present in human blood and lymphoid tissue. (A): Flow cytometry analysis of $CXCR5^+$ $CXCR3^-$ and $CXCR5^+$ $CXCR3^+$ CD4 T cells from blood (n=14), tonsil (n=8) and lymph node (n=7) compartments from HIV-1 negative donors. Representative dot plots are shown on the left with numbers in quadrants representing percentages of different cell subsets. Right panel shows cumulative data from peripheral blood (P. Blood, n=14), tonsil (n=8) and lymph node (n=7). Statistical significance was calculated using a two-tailed Wilcoxon matched-pairs signed rank test (*p<0.05). (B): Flow cytometric gating of $CXCR3^+$ $PD\text{-}1^{Lo}$ (green), $CXCR3^+$ $PD\text{-}1^{Hi}$ (garnet), $CXCR3^-$ $PD\text{-}1^{Lo}$ (brown) and $CXCR3^-$ $PD\text{-}1^{Hi}$ (orange) CD4 T cells from indicated tissue compartments (left panel). Right panel summarizes the proportions of these cell subsets within CD4 T cells from each compartment; P. Blood, tonsil and lymph node. Statistical significance was calculated using a Friedman test followed by a Dunn's test (*p<0.05; **p<0.01; ***p<0.001).

Supplemental Figure 2. Phenotypical and functional analysis of mDC-primed Tfh-like cells. (A): Overlay histograms reflecting Bcl-6, ICOS, Foxp3, CXCR3 and Tbet expression in gated $PD\text{-}1^{Lo}$ (orange) and $PD\text{-}1^{Hi}$ (blue) $CXCR5^+$ CD4 T cells defined as in panel A. $CXCR5^-$ $PD\text{-}1^-$ CD4 T cells (black) as internal controls and unstained background for each gated population are shown in open histograms. (B): Tbet expression levels in CD4 T cells cultured with B cells in the presence or absence of mDCs, or with LPS-activated mDCs alone (n=8). Statistical significance among different conditions was calculated using a Friedman test followed by a Dunn's test (*p<0.05; **p<0.01). (C) Proportions of $PD\text{-}1^{Lo}$ (left) and $PD\text{-}1^{Hi}$ (right) Tfh-like cells generated in the presence of autologous naïve B cells and allogeneic mDCs isolated from HIV-1 negative lymph nodes (n=3). (D): Concentrations of indicated cytokines in supernatants from naïve B cells co-cultured for 7 days with autologous naïve T cells from HIV-1 negative donors in the absence (violet) or presence of allogeneic mDCs from HIV-1 negative (NG, n=11), controller non-neutralizers (NN, n=16) and neutralizers (NT, n=16), untreated (CP, n=10) and HAART-treated (H) chronic progressors. Statistical significance between DC from NT and other conditions was calculated using a Kruskal-Wallis test followed by a Dunn's test (*p<0.05; **p<0.01; ***p<0.01).

Supplemental Figure 3. B cell phenotypical and functional analysis on Tfh priming assays. (A): Representative flow cytometric analysis of CD38 vs CD27 expression on gated $CD19^+$ B cells co-cultured with autologous T cells alone or with allogeneic cDCs from either HIV-1 negative persons (NG, n=11), controller non-neutralizers (NN, n=16), neutralizers (NT, n=16), untreated HIV patients (CP, n=10) or HAART-treated (H, n=10) chronic progressors. Numbers represent proportions of cells within each gate. (B): Proportions of $CD38^{Lo/-}$ $CD27^+$ resting memory, $CD38^{Hi}$ $CD27^{Hi}$ Plasmablast-like, $CD38^{Int}$ $CD27^{Int}$ activated memory and $CD38^+CD27^-$ transitional-like B cells defined as in (A) and generated in the absence or presence of autologous T cells and allogeneic mDCs from the different study cohorts.

Statistical significance of differences between mDCs from NT and mDCs from all other cohorts or control T and B cells alone was calculated using a Kruskal-Wallis test followed by a Dunn's test (*p<0.05). (C): Luminex analysis of concentrations of IgM, IgA and IgGs in supernatants used in (B) from the indicated co-culture conditions. Contributions of IgG to total Igs are shown on the far right panel. Statistical significance of differences between DC from NT and all others was calculated and corrected for multiple comparisons using a Kruskal-Wallis test followed by a Dunn's test (*p<0.05; **p<0.01).

Supplemental Figure 4. Molecular mechanisms underlying in vitro mDC-mediated priming of Tfh-like cells. (A): Proportions of CXCR5^{+} PD-1^{+} (left), Bcl-6^{+} PD-1^{+} (middle) and ICOS^{Hi} PD-1^{+} (right) CD4 T cells cultured in the absence or the presence of autologous B cells and allogeneic mDCs in the same (no parenthesis) or in a different (between parenthesis) transwell compartment (n=4). Statistical significance was calculated using a Friedman test followed by a Dunn's test (*p<0.05). (B): Mean Fluorescence Intensity of CD86 and PD-L1 in gated mDCs from HIV+ controller non-neutralizers (NN; n=18) and neutralizers (NT; n=24).

Supplemental Figure 5. Phenotypical characterization of pheripheral blood and lymphoid tissue Tfh-like. Flow cytometric analysis of surface expression of ICOS and intracellular Bcl-6 expression on gated CD4 T cells expressing either low (PD-1^{Lo}) or high (PD-1^{Hi}) levels of PD-1 in CXCR3^{-} and CXCR3^{+} CXCR5^{+} Tfh-like subpopulations from peripheral blood (P.Blood; (P.Blood; ICOS n=6 and Bcl=6 n=9; upper panel), tonsils (middle panel; n=8) and lymph nodes (lower panels; n=6). Numbers represent the percentages of cells within each quadrants. Summary of mean fluorescence intensities of ICOS and Bcl-6 in different experiments are shown on the right. Statistical significance of differences among populations was calculated using a Friedman test followed by a Dunn's test (*p<0.05;**p<0.01, ***p<0.001).

Supplemental Figure 6. Functional analysis of pTfh cells inducing B cell activation, cytokine secretion and production of Immunoglobulins. (A): Proportions of CD38^{-} CD27^{+} resting memory and CD38^{+} CD27^{-} transitional B cells on day 6 of co-culture with indicated pTfh populations. CXCR3^{+} PD-1^{Lo} (n=5), CXCR3^{+} PD-1^{Hi} (n=5), CXCR3^{-} PD-1^{Lo} (n=4) and CXCR3^{-} PD-1^{Hi} (n=5). (B-C): Luminex analysis of indicated cytokine (B) and IgG subclass (C) concentrations present in supernatants on day 6 in the indicated co-cultures of B cells alone or with CXCR3^{+} PD-1^{Lo} (n=5), CXCR3^{+} PD-1^{Hi} (n=5), CXCR3^{-} PD-1^{Lo} (n=4) and CXCR3^{-} PD-1^{Hi} (n=5) pTfh. Statistical significance among the 5 conditions was calculated using a Kruskal-Wallis test followed by a Dunn's test (*p< 0.05; **p<0.01).

Supplemental Figure 7. Analysis of T cell memory subsets in circulating Tfh-like cell subpopulations from the blood of HIV-1 controller neutralizers and non neutralizers. (A): Proportions of naïve (NA), stem cell memory (SCM), central memory (CM), effector memory (EM), terminally differentiated (TD) cells defined by CCR7 vs CD45RO expression as shown in Figure 5A within CXCR3^{+} PD-1^{Lo} (green)

and PD-1^{Hi} (garnet), CXCR3^{-} PD-1^{Lo} (brown) and PD-1^{Hi} (orange) and total CD4 T cells (CD4, black) from peripheral blood from HIV controller neutralizers (NT, n=20, lower row) and non-neutralizers (NN, n=18, upper row). Statistical differences in memory subset composition within each pTfh subpopulation were calculated using a Friedman test followed by a Dunn's test (*p<0.05; **p<0.01, ***p<0.001). (B): Distributions of SCM are also represented individually within each pTfh subpopulation comparing NN (n=18) and NT (n=20). Statistical differences in T_{SCM} proportions between HIV controller neutralizers and non-neutralizers within each PD-1^{Lo} and PD-1^{Hi} pTfh subset was calculated using a one-tailed Mann Whitney test (*p<0.05, red).

Supplemental Figure 8. Viability and proliferative capacity of different Tfh-like cell subpopulations from human blood. (A): Histograms (left panel) show representative flow cytometric analysis of CFSE dilution on sorted pTfh subpopulations on day 6 of culture with autologous B cells and SEB. Black dash lines reflect CFSE levels of control cells cultured with media alone. Numbers within histograms correspond to proportions of proliferating cells. Right panel summarizes proportions of proliferating cells in sorted pTfh subpopulations on day 6 (n=3). (B): Representative flow cytometric analysis showing CFSE dilution on gated PD-1^{Lo} and PD-1^{Hi} cells on day 6 of culture of sorted CXCR5^{+} CXCR3^{+} PD-1^{Lo} T cells with B cells and SEB. (C): summary the proportions of proliferating PD-1^{Lo} and PD-1^{Hi} cells in n=3 experiments. (D): Proliferative activity of CXCR5^{+} CXCR3^{+} PD-1^{Lo} cells assessed in serial culture experiments. PD-1^{Lo} cells isolated on day 6 are highlighted in blue; PD-1^{Lo} cells resorted on day 6 and cultured for six additional days are highlighted in green. Numbers in the histogram represent proportion of proliferating cells from corresponding populations. Unstimulated cells are shown in black dash line.

Figure 1.

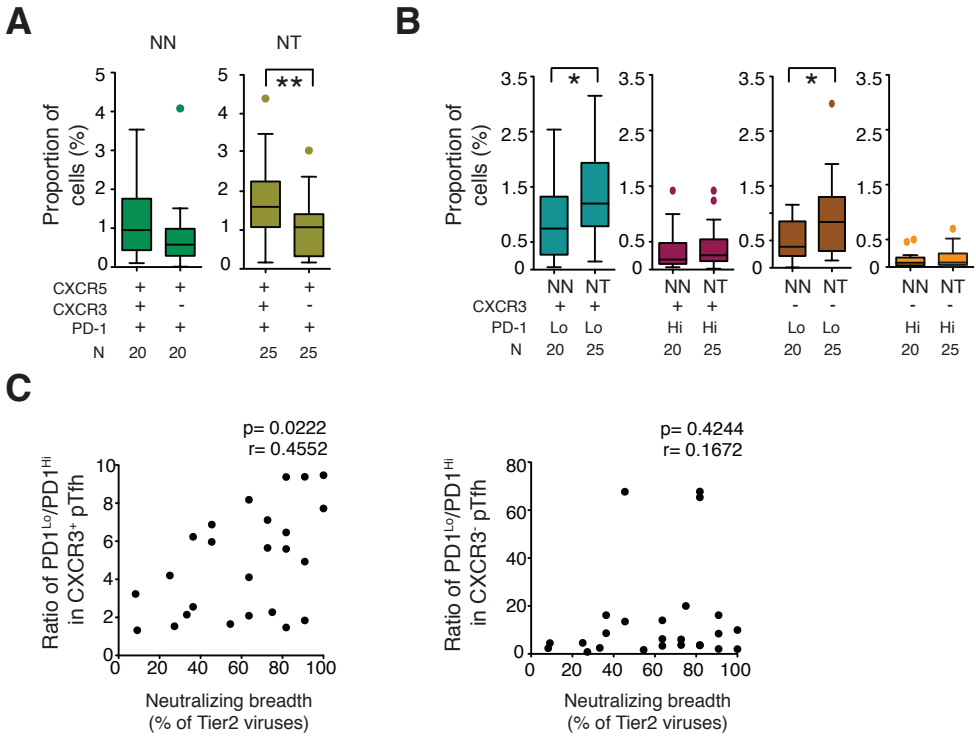

Figure 1. CXCR5⁺ CXCR3⁺ PD-1^{Lo} Tfh-like cells are enriched in controller neutralizers and associated with neutralizing breadth against HIV-1. (A): Proportions of total CXCR3⁺ PD-1⁺ CXCR5⁺ or CXCR3⁻ PD-1⁺ CXCR5⁺ subpopulations within total CD4 T cells in the blood from HIV-infected controller non-neutralizers (NN, n=20) and neutralizers (NT, n=25). Statistical differences were calculated using a Wilcoxon matched-pairs test in each group of patients (**p<0.01). (B): Proportions of PD-1^{Lo} or PD-1^{Hi} cells within CXCR3⁺ CXCR5⁺ and CXCR3⁻ CXCR5⁺ CD4 T cell populations from indicated study cohorts. Statistical differences between NN and NT were calculated separately for each individual pTfh subset using a Mann Whitney U test (* p<0.05). (C): Spearman correlations between ratios of PD-1^{Lo} vs PD-1^{Hi} cells within CXCR3⁺ (left) and CXCR3⁻ (right) CXCR5⁺ CD4 T cells from controller neutralizers and the corresponding breadth of HIV-1-specific neutralizing antibodies. Numbers included on the top right corner of each plot reflect nominal P-values and spearman R values.

Figure 2.

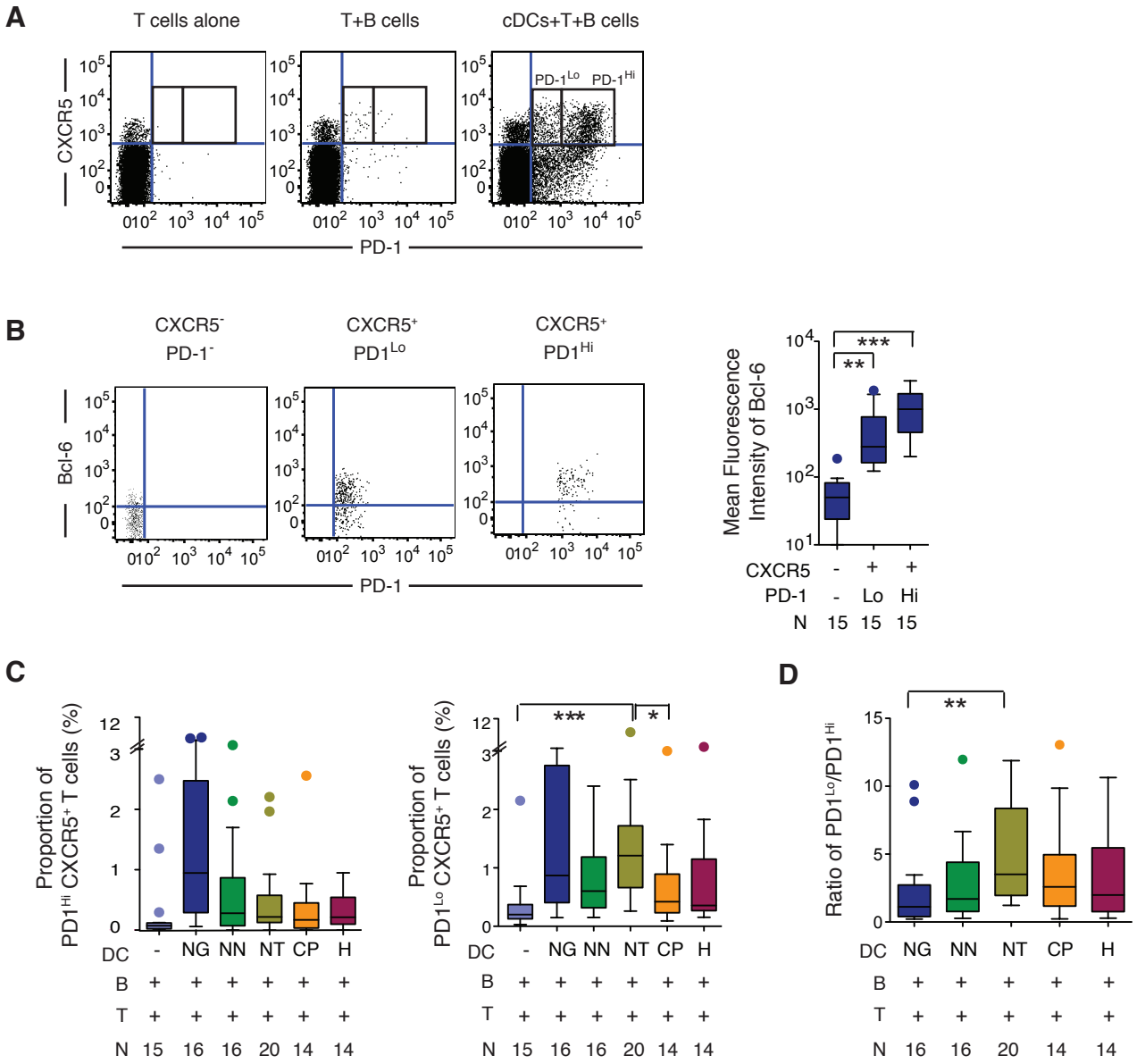

Figure 2. Primary mDCs from controller neutralizers efficiently induce Tfh-like cells *in vitro*. (A): Flow cytometry analysis of CXCR5 and PD-1 expression on naive CD4 T cells from an HIV-1 negative donor cultured for 7 days in the presence of media alone (left) or autologous naïve B cells in the absence (middle) or the presence (right) of allogeneic mDCs isolated from an additional HIV-1 negative donor. Rectangles highlight CXCR5$^+$ CD4 T cells expressing either low or high levels of PD-1 (PD-1^{Lo} and PD-1^{Hi}, respectively). Dot plots from a representative experiment are shown. (B): Intracellular Bcl-6 expression in indicated CD4 T cell subsets after co-culture with mDCs for 7 days. Left panel shows flow cytometry plots from one representative experiment. Right panel shows cumulative mean fluorescence intensity of Bcl-6 data from n=15 HIV-1 negative study subjects. Statistical significance was calculated using a Friedman test followed by a Dunn's test (**p< 0.01; ***p<0.001). (C): Proportions of PD-1^{Hi} (left) and PD-1^{Lo} (right) CXCR5$^+$ CD4 T cells differentiated from naïve CD4 T cells after 7 days of culture in the presence of autologous naïve B cells (violet) alone or in combination with allogeneic mDCs from HIV-1 negative donors (NG; blue, n=16), controller non-neutralizers (NN; dark green n=16) and neutralizers (NT; light green n=20), untreated (CP; orange n=14) and HAART-treated (H; purple n=14) chronic progressors. Statistical significance between NT and all other conditions was calculated using a Kruskal-Wallis test followed by a Dunn's test (*p<0.05; ***p<0.001). (D): Ratios of PD-1^{Lo} vs PD-1^{Hi} CXCR5$^+$ CD4 T cells differentiated in the presence of allogeneic mDCs from different study cohorts. Statistical significance between NT vs all other conditions was calculated using a Kruskal-Wallis test followed by a Dunn's test (**p<0.01).

Figure 3.

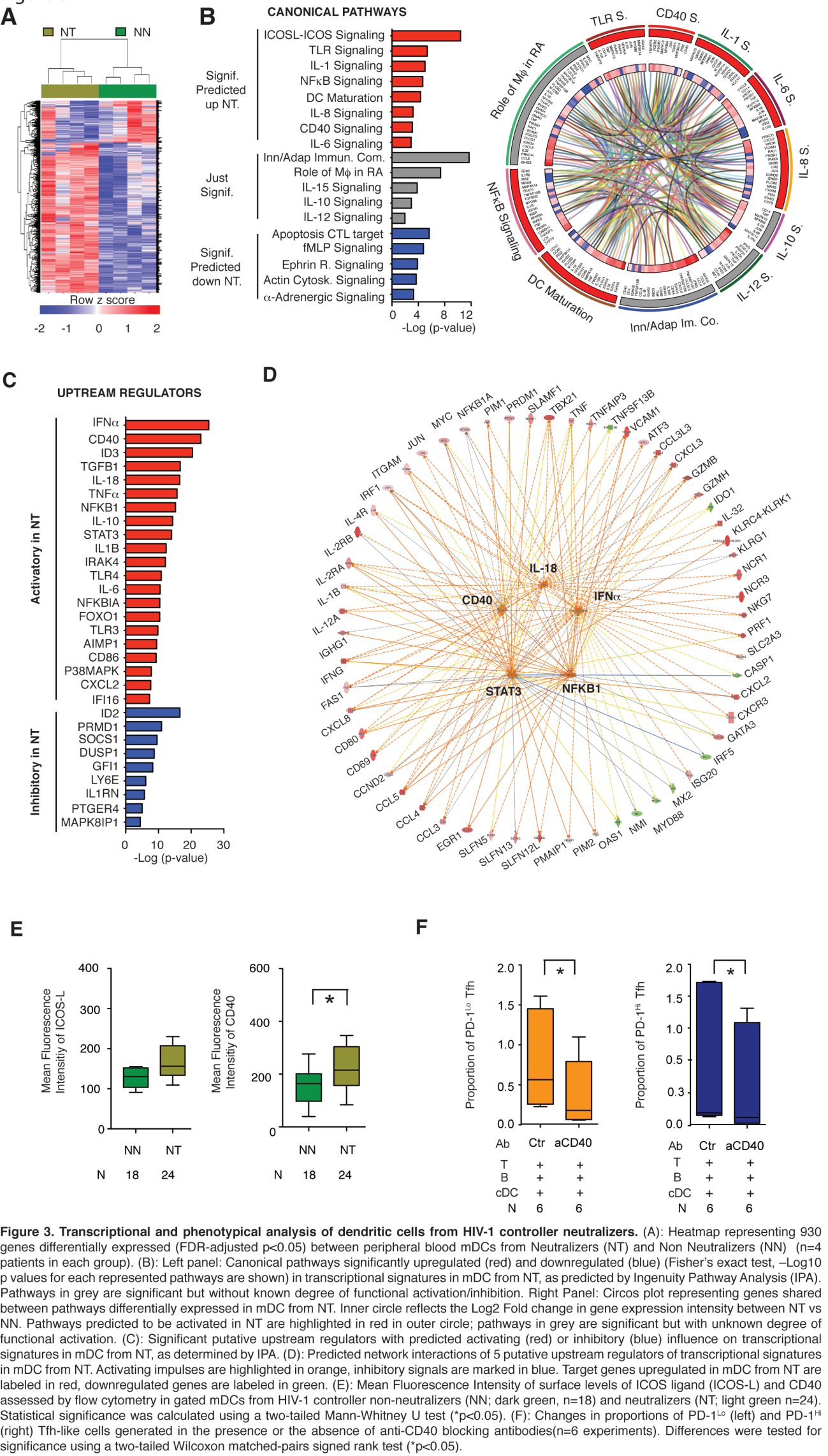

Figure 3. Transcriptional and phenotypical analysis of dendritic cells from HIV-1 controller neutralizers. (A): Heatmap representing 930 genes differentially expressed (FDR-adjusted p<0.05) between peripheral blood mDCs from Neutralizers (NT) and Non Neutralizers (NN) (n=4 patients in each group). (B): Left panel: Canonical pathways significantly upregulated (red) and downregulated (blue) (Fisher's exact test, –Log10 p values for each represented pathways are shown) in transcriptional signatures in mDC from NT, as predicted by Ingenuity Pathway Analysis (IPA). Pathways in grey are significant but without known degree of functional activation/inhibition. Right Panel: Circos plot representing genes shared between pathways differentially expressed in mDC from NT. Inner circle reflects the Log2 Fold change in gene expression intensity between NT vs NN. Pathways predicted to be activated in NT are highlighted in red in outer circle; pathways in grey are significant but with unknown degree of functional activation. (C): Significant putative upstream regulators with predicted activating (red) or inhibitory (blue) influence on transcriptional signatures in mDC from NT, as determined by IPA. (D): Predicted network interactions of 5 putative upstream regulators of transcriptional signatures in mDC from NT. Activating impulses are highlighted in orange, inhibitory signals are marked in blue. Target genes upregulated in mDC from NT are labeled in red, downregulated genes are labeled in green. (E): Mean Fluorescence Intensity of surface levels of ICOS ligand (ICOS-L) and CD40 assessed by flow cytometry in gated mDCs from HIV-1 controller non-neutralizers (NN; dark green, n=18) and neutralizers (NT; light green n=24). Statistical significance was calculated using a two-tailed Mann-Whitney U test (*p<0.05). (F): Changes in proportions of PD-1^{Lo} (left) and PD-1^{Hi} (right) Tfh-like cells generated in the presence or the absence of anti-CD40 blocking antibodies(n=6 experiments). Differences were tested for significance using a two-tailed Wilcoxon matched-pairs signed rank test (*p<0.05).

Figure 4.

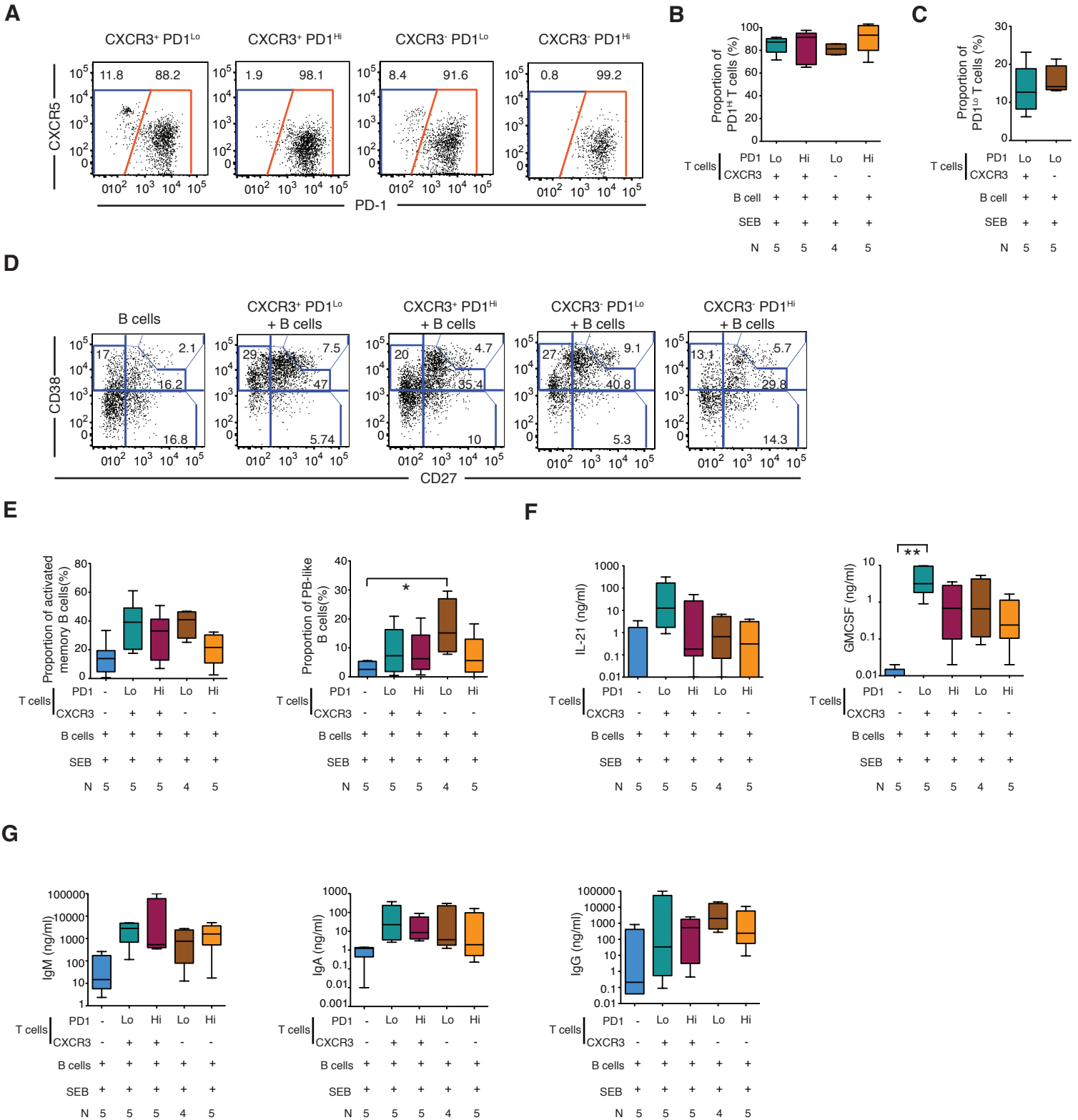

Figure 4. CXCR3⁺ PD-1^{Lo} pTfh cells support B cell activation and differentiation. (A): Dot plots reflect CXCR5 vs PD-1 expression on sorted CXCR3⁺ and CXCR3⁻ PD-1^{Lo} and PD-1^{Hi} pTfh cells on day 6 in co-culture with autologous total B cells in the presence of SEB in a representative experiment. Numbers above the gates represent percentages of cells. (B-C): Proportions of PD-1^{Hi} (B) and PD-1^{Lo} (C) CD4 T cells after six-day culture of isolated CXCR3⁺ PD-1^{Lo} (n=5), CXCR3⁺ PD-1^{Hi} (n=5), CXCR3⁻ PD-1^{Lo} (n=4) and CXCR3⁻ PD-1^{Hi} (n=5) cells with autologous B cells and SEB. (D): Representative flow cytometry analysis showing CD38 vs CD27 surface expression on gated CD19⁺ B cells on day 6 of co-culture with SEB alone or the indicated pTfh populations. Numbers within the gates represent percentages of cells. (E): Proportions of CD38^{Int} CD27^{Int} activated memory and CD38^{Hi} CD27^{Hi} plasmablast-like B cells on day 6 of co-culture with indicated pTfh populations. CXCR3⁺ PD-1^{Lo} (n=5), CXCR3⁺ PD-1^{Hi}(n=5), CXCR3⁻ PD-1^{Lo} (n=4) and CXCR3⁻ PD-1^{Hi} (n=5). Differences between each condition with indicated pTfh subset and control B cells activated with SEB alone were tested for statistical significance using a Kruskal-Wallis test followed by Dunn's test (*p<0.05). (F-G): Luminex analysis of indicated cytokine (F) and Ig (G) concentrations present in supernatants on day 6 in the indicated co-cultures with CXCR3⁺ PD-1^{Lo} (n=5), CXCR3⁺ PD-1^{Hi} (n=5), CXCR3⁻ PD-1^{Lo} (n=4) and CXCR3⁻ PD-1^{Hi} (n=5) pTfh. Statistical significance was calculated using a Kruskal-Wallis test followed by a Dunn's test (**p<0.01).

Figure 5.

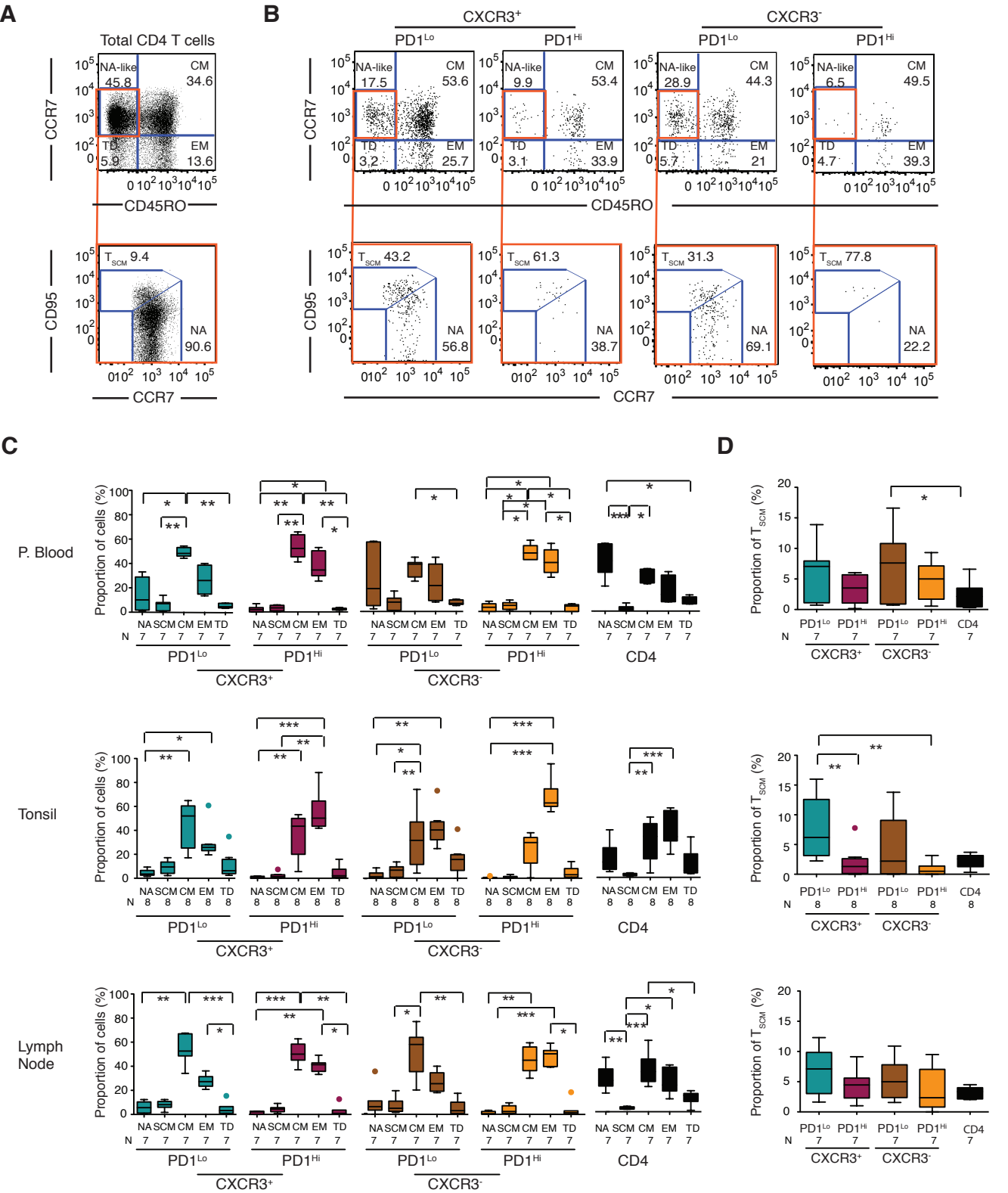

Figure 5. Characterization of memory cell subsets within Tfh-like cells. (A-B): Representative flow cytometry analysis of memory cell subsets in total CD4 T cells (A) and in PD-1^{Lo} and PD-1^{Hi} CXCR5^{+} CXCR3^{+} and CXCR5^{+} CXCR3^{-} pTfh cells (B). CCR7 vs CD45RO expression define central memory (CM), effector memory (EM), terminally differentiated (TD) and naïve-like (NA-like) T cells (upper panels). NA-like T cells are subdivided into memory stem cells (SCM) and naïve (NA) cells based on expression levels of CD95 (lower panels). (C-D) Proportions of memory subsets within PD-1^{Lo} and PD-1^{Hi} CXCR3^{+} and CXCR3^{-} cells, and total CD4 T cells (CD4) from peripheral blood (P. Blood; upper panel, n=7), tonsils (middle panel, n=8) and lymph nodes (lower panel, n=7) (C). Proportions of T memory stem cells (SCM) within each pTfh subset from the indicated compartments are represented separately in (D). Statistical significance within individual subset (C) and in T_{SCM} proportions across different subsets (D) was calculated using a Friedman test followed by a Dunn's test (*p<0.05; **p<0.01; ***p<0.001).

Figure 6.

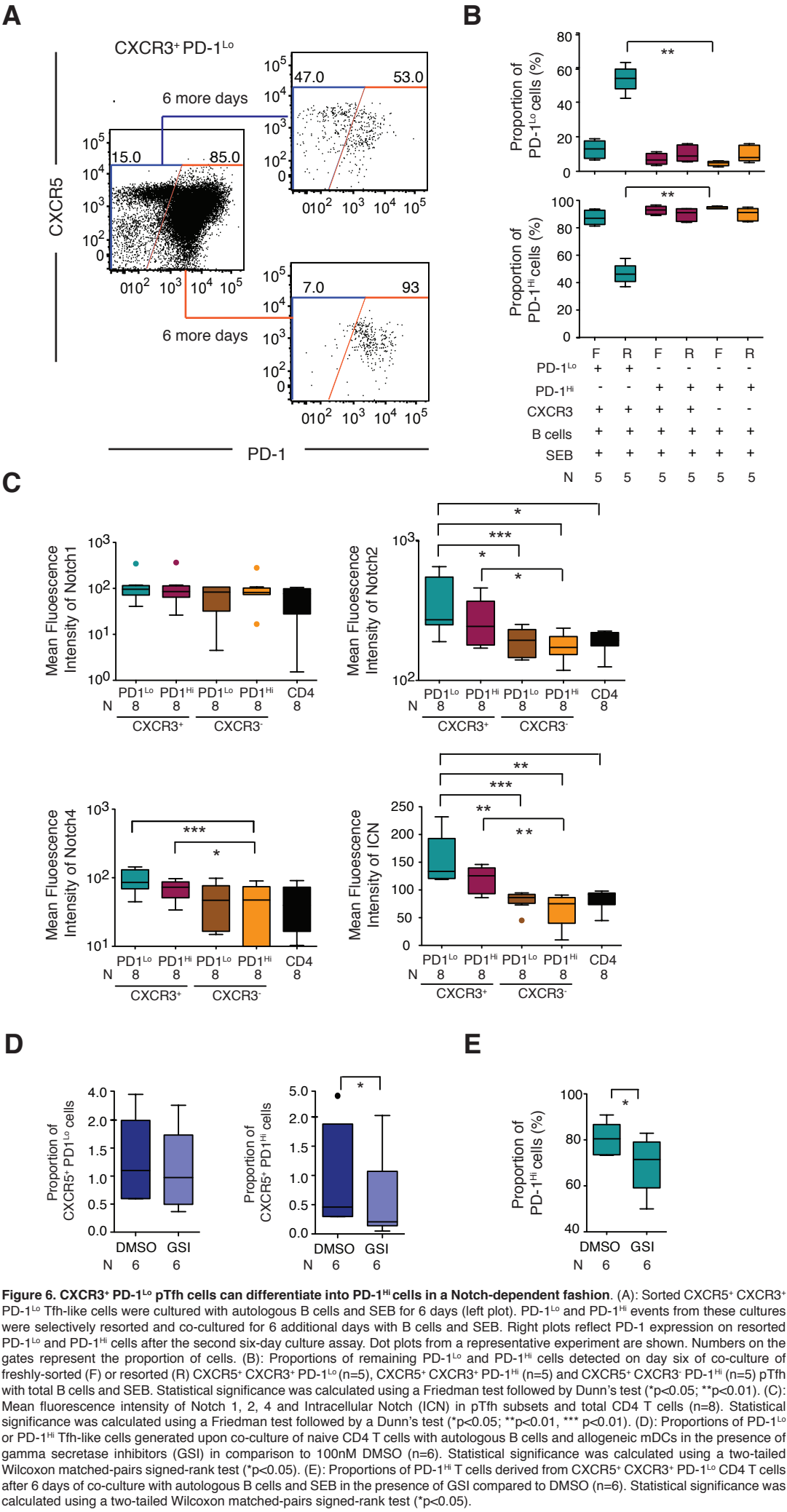

Figure 6. CXCR3⁺ PD-1^{Lo} pTfh cells can differentiate into PD-1^{Hi} cells in a Notch-dependent fashion. (A): Sorted CXCR5⁺ CXCR3⁺ PD-1^{Lo} Tfh-like cells were cultured with autologous B cells and SEB for 6 days (left plot). PD-1^{Lo} and PD-1^{Hi} events from these cultures were selectively resorted and co-cultured for 6 additional days with B cells and SEB. Right plots reflect PD-1 expression on resorted PD-1^{Lo} and PD-1^{Hi} cells after the second six-day culture assay. Dot plots from a representative experiment are shown. Numbers on the gates represent the proportion of cells. (B): Proportions of remaining PD-1^{Lo} and PD-1^{Hi} cells detected on day six of co-culture of freshly-sorted (F) or resorted (R) CXCR5⁺ CXCR3⁺ PD-1^{Lo} (n=5), CXCR5⁺ CXCR3⁺ PD-1^{Hi} (n=5) and CXCR5⁺ CXCR3⁻ PD-1^{Hi} (n=5) pTfh with total B cells and SEB. Statistical significance was calculated using a Friedman test followed by Dunn's test (*p<0.05; **p<0.01). (C): Mean fluorescence intensity of Notch 1, 2, 4 and Intracellular Notch (ICN) in pTfh subsets and total CD4 T cells (n=8). Statistical significance was calculated using a Friedman test followed by a Dunn's test (*p<0.05; **p<0.01, *** p<0.01). (D): Proportions of PD-1^{Lo} or PD-1^{Hi} Tfh-like cells generated upon co-culture of naive CD4 T cells with autologous B cells and allogeneic mDCs in the presence of gamma secretase inhibitors (GSI) in comparison to 100nM DMSO (n=6). Statistical significance was calculated using a two-tailed Wilcoxon matched-pairs signed-rank test (*p<0.05). (E): Proportions of PD-1^{Hi} T cells derived from CXCR5⁺ CXCR3⁺ PD-1^{Lo} CD4 T cells after 6 days of co-culture with autologous B cells and SEB in the presence of GSI compared to DMSO (n=6). Statistical significance was calculated using a two-tailed Wilcoxon matched-pairs signed-rank test (*p<0.05).

Supplemental Figure 1.

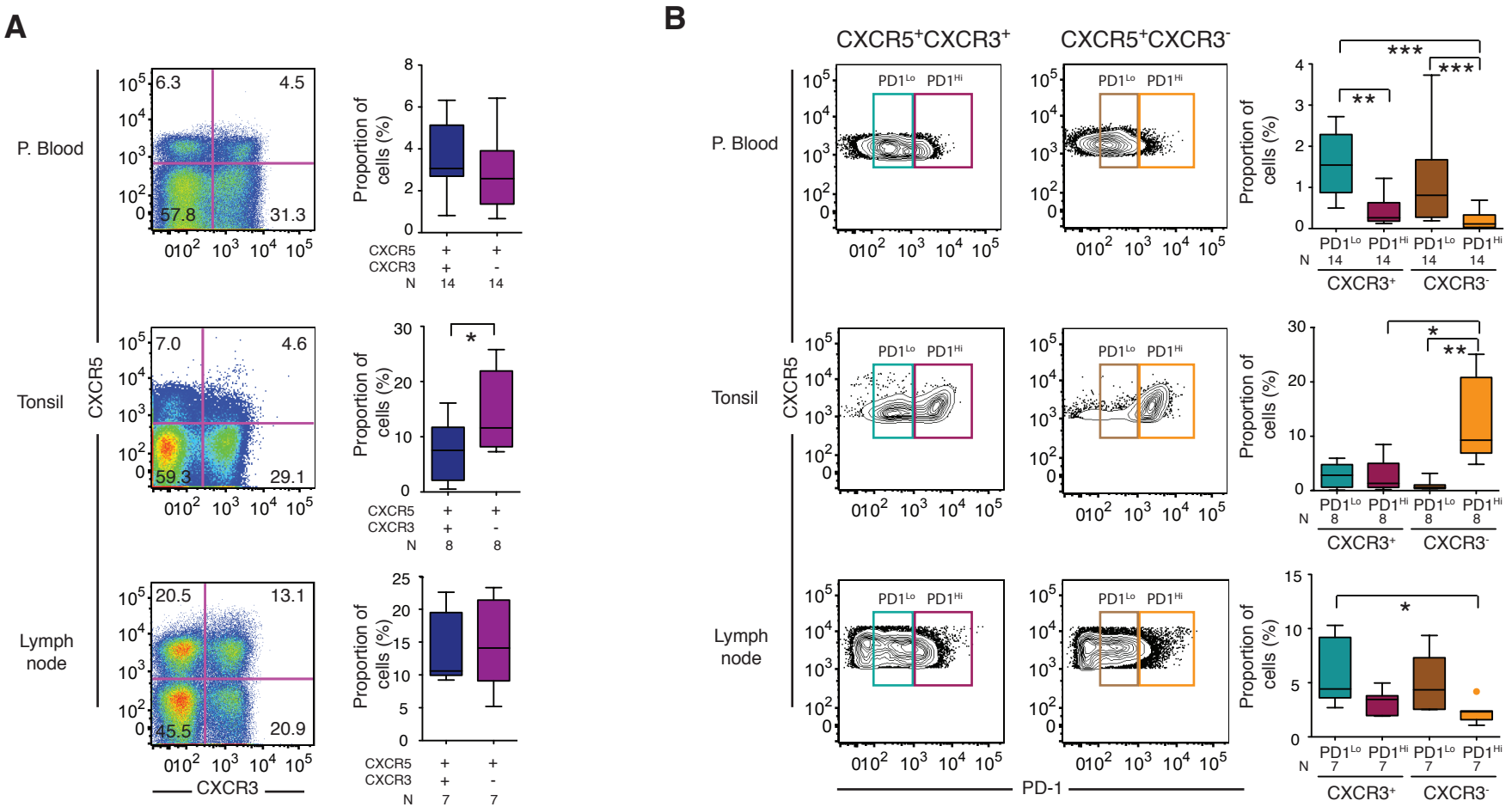

Supplemental Figure 1. CXCR3 and PD-1 expression defines Tfh-like subsets present in human blood and lymhoid tissue. (A): Flow cytometry analysis of CXCR5$^+$ CXCR3$^-$ and CXCR5$^+$ CXCR3$^+$ CD4 T cells from blood (n=14), tonsil (n=8) and lymph node (n=7) compartments from HIV-1 negative donors. Representative dot plots are shown on the left with numbers in quadrants representing percentages of different cell subsets. Right panel shows cumulative data from peripheral blood (P. Blood, n=14), tonsil (n=8) and lymph node (n=7). Statistical significance was calculated using a two-tailed Wilcoxon matched-pairs signed rank test (*p<0.05). (B): Flow cytometric gating of CXCR3$^+$ PD-1^{Lo} (green), CXCR3$^+$ PD-1^{Hi} (garnet), CXCR3$^-$ PD-1^{Lo} (brown) and CXCR3$^-$ PD-1^{Hi} (orange) CD4 T cells consistently from indicated tissue compartments (left panel). Right panel summarizes the proportions of these cell subsets within CD4 T cells from each compartment; P. Blood, tonsil and lymph node. Statistical significance was calculated using a Friedman test followed by a Dunn's test (*p<0.05; **p<0.01;

Supplemental Figure 2.

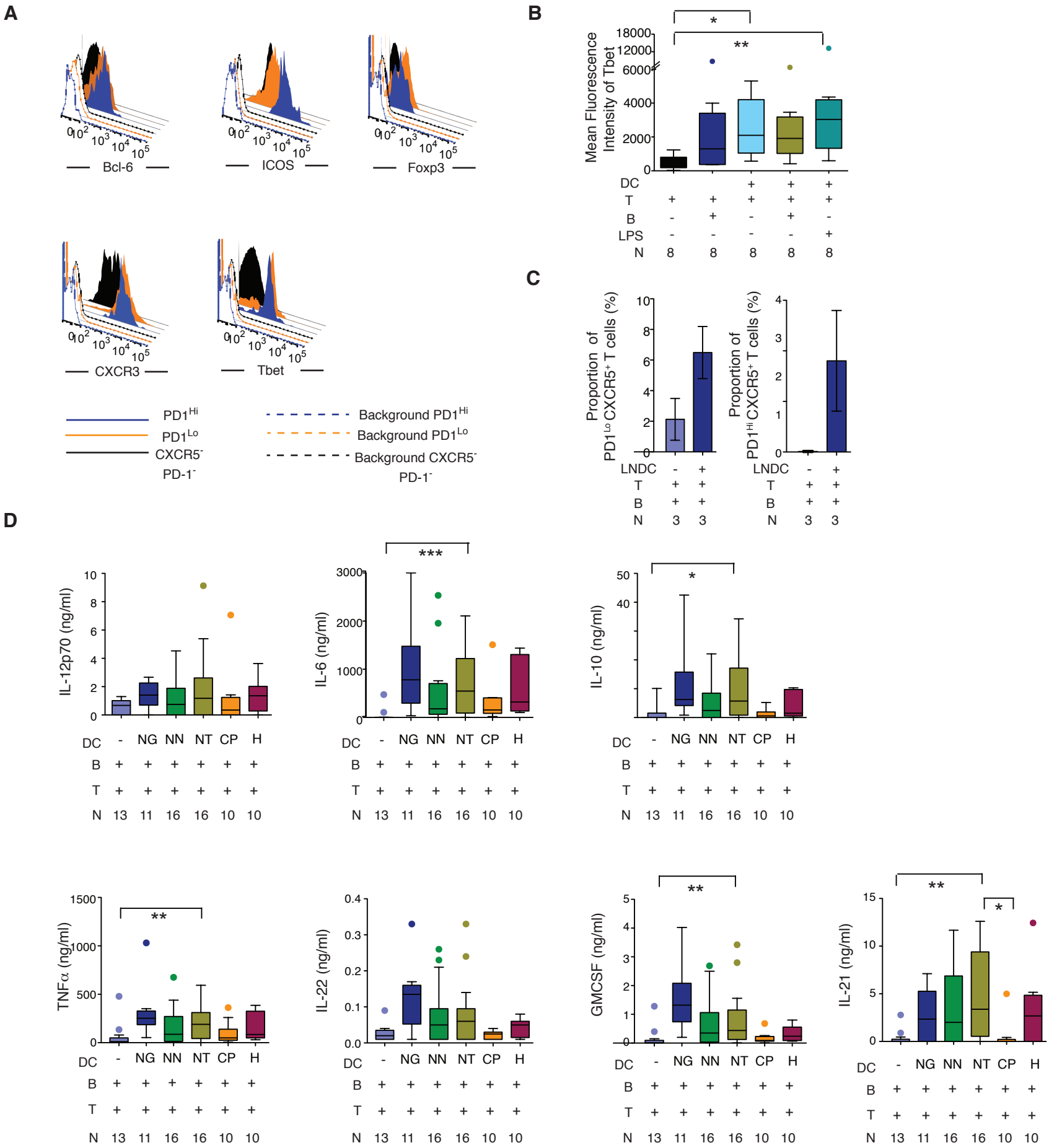

Supplemental Figure 2. Phenotypical and functional analysis of mDC-primed Tfh-like cells. (A): Overlay histograms reflecting Bcl-6, ICOS, Foxp3, CXCR3 and Tbet expression in gated PD-1^{Lo} (orange) and PD-1^{Hi} (blue) CXCR5^{+} CD4 T cells defined as in panel A. CXCR5^{-} PD-1^{-} CD4 T cells (black) as internal controls and unstained background for each gated population are shown in open histograms. (B): Tbet expression levels in CD4 T cells cultured with B cells in the presence or absence of mDCs, or with LPS-activated mDCs alone (n=8). Statistical significance among different conditions was calculated using a Friedman test followed by a Dunn's test (*p<0.05; **p<0.01). (C) Proportions of PD-1^{Lo} (left) and PD-1^{Hi} (right) Tfh-like cells generated in the presence of autologous naïve B cells and allogeneic mDCs isolated from HIV-1 negative lymph nodes (n=3). (D): Concentrations of indicated cytokines in supernatants from naïve B cells co-cultured for 7 days with autologous naïve T cells from HIV-1 negative donors in the absence (violet) or presence of allogeneic mDCs from HIV-1 negative (NG; n=11), controller non-neutralizers (NN; n=16) and neutralizers (NT; n=16), untreated (CP; n=10) and HAART-treated (H; n=10) chronic progressors. Statistical significance between NT and all other conditions was calculated using a Kruskal-Wallis test followed by a Dunn's test (*p<0.05; **p<0.01; ***p<0.01).

Supplemental Figure 3.

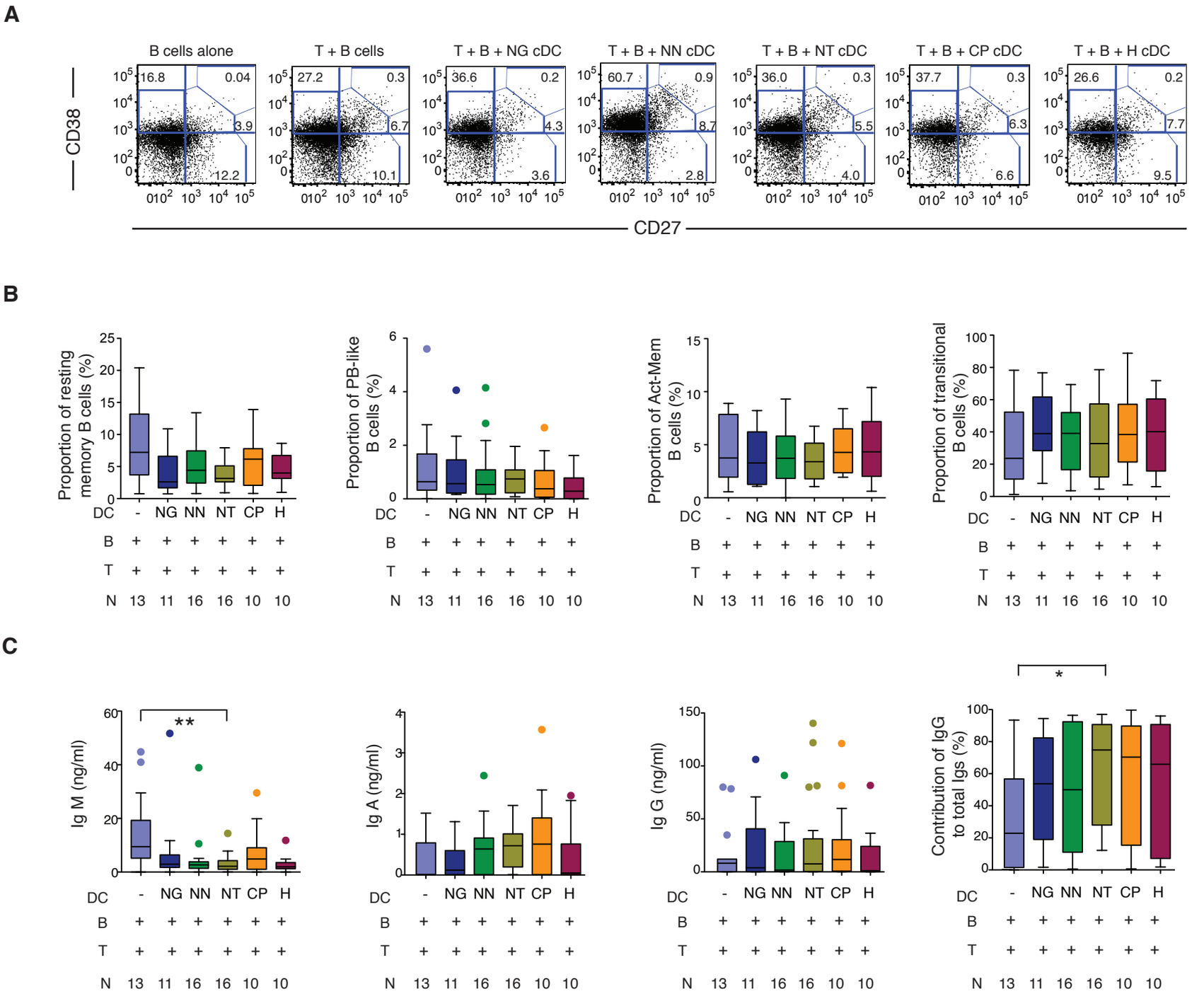

Supplemental Figure 3. B cell phenotypical and functional analysis on Tfh priming assays. (A): Representative flow cytometric analysis of CD38 vs CD27 expression on gated CD19^{+} B cells co-cultured with autologous T cells alone (violet; n=13) or allogeneic mDCs from either HIV-1 negative (NG; n=11), controller non-neutralizers (NN; n=16) and neutralizers (NT; n=16), untreated (CP; n=10) and HAART-treated (H; n=10) chronic progressors. Numbers represent proportions of cells within each gate. (B): Proportions of CD38$^{Lo/-}$ CD27^{+} resting memory, CD38^{Hi} CD27^{Hi} Plasmablast-like, CD38^{Int} CD27^{Int} activated memory and CD38^{+}CD27^{-} transitional-like B cells defined as in (A) and generated in the absence or presence of autologous T cells and allogeneic mDCs from the different study cohorts. Statistical significance of differences between mDCs from NT and mDCs from all other cohorts or control T and B cells alone was calculated using a Kruskal-Wallis test followed by a Dunn's test (*p<0.05). (C): Luminex analysis of concentrations of IgM, IgA and IgGs in supernatants used in (B) from the indicated co-culture conditions. Contributions of IgG to total Igs are shown on the far right panel. Statistical significance of differences between NT and all others for each plot in B and C was calculated and corrected for multiple comparisons using a Kruskal-Wallis test followed by a Dunn's test (*p<0.05; **p<0.01).

Supplemental Figure 4.

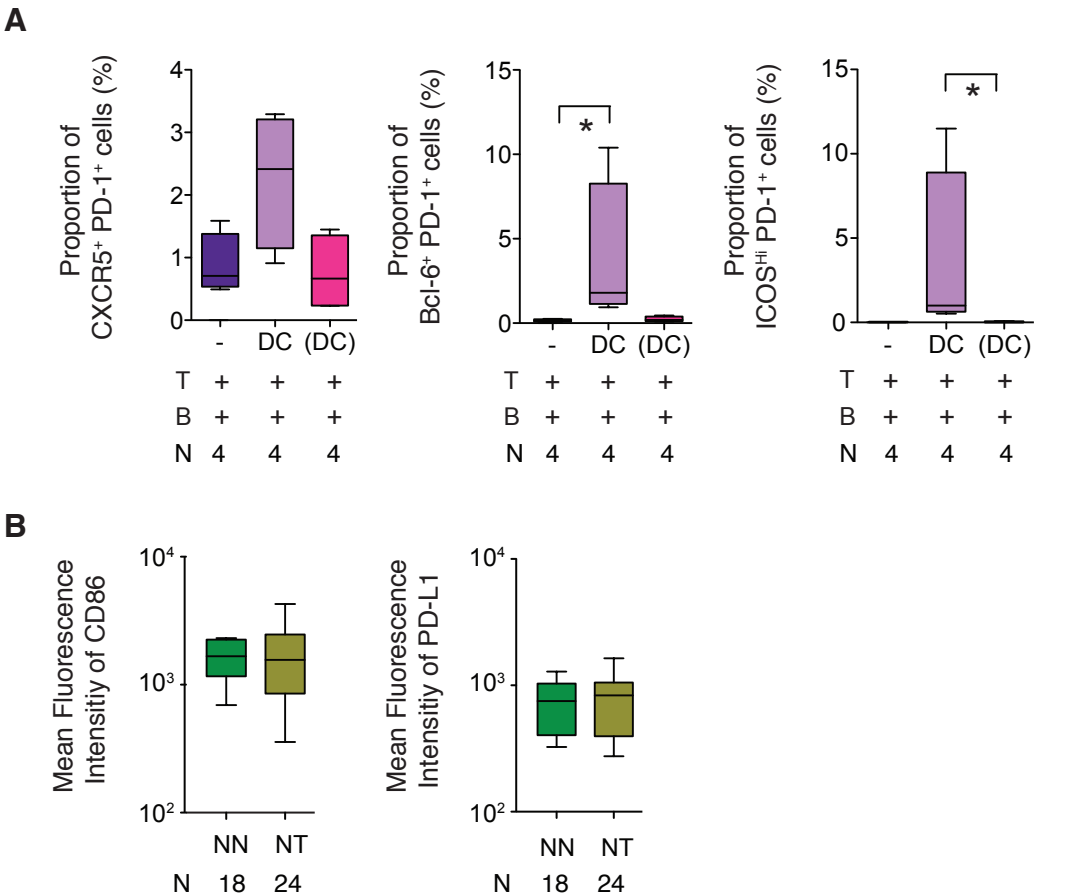

Supplemental Figure 4. Molecular mechanisms underlying in vitro mDC-mediated priming of Tfh-like cells. (A): Proportions of CXCR5^{+} PD-1^{+} (left), Bcl-6^{+} PD-1^{+} (middle) and ICOS^{Hi} PD-1^{+} (right) CD4 T cells cultured in the absence or the presence of autologous B cells and allogeneic mDCs in the same (no parenthesis) or in a different (between parenthesis) transwell compartments (n=4). Statistical significance was calculated using a Friedman test followed by a Dunn's test (*p<0.05). (B): Mean Fluorescence Intensity of CD86 and PD-L1 in gated mDCs from HIV^{+} controller non-neutralizers (NN; n=18) and neutralizers (NT; n=24).

Supplemental Figure 5.

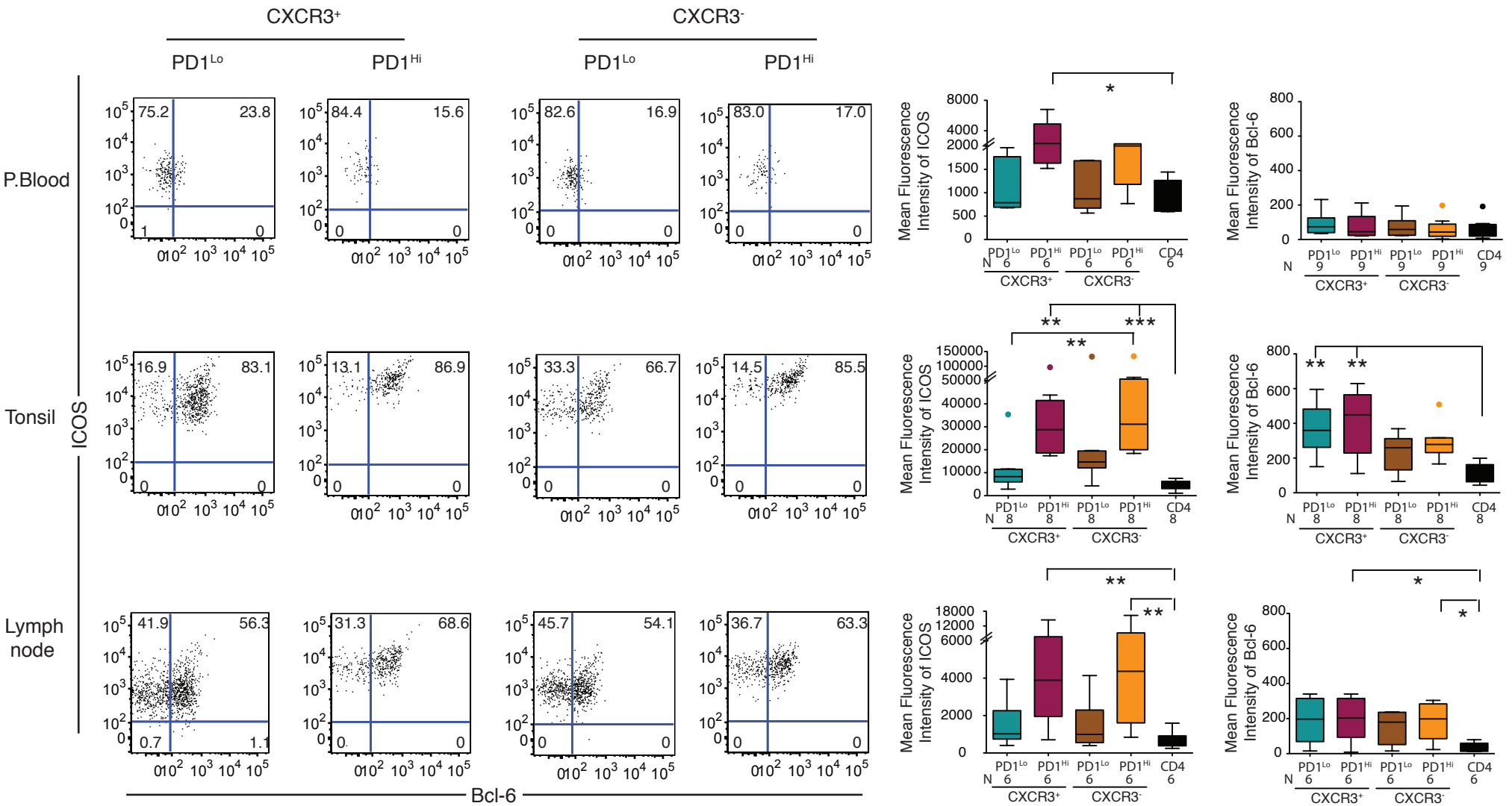

Supplemental Figure 5. Phenotypical characterization of pheripheral blood and lymphoid tissue Tfh-like subsets. Flow cytometric analysis of surface expression of ICOS and intracellular Bcl-6 expression on gated CD4 T cells expressing either low (PD-1^{Lo}) or high (PD-1^{Hi}) levels of PD-1 in CXCR3^{-} and CXCR3^{+} CXCR5^{+} Tfh-like subpopulations from peripheral blood (P.Blood; ICOS n=6 and Bcl=6 n=9; upper panel), tonsils (middle panel; n=8) and lymph nodes (lower panels; n=6). Numbers in quadrants represent the percentages of cells within quadrants. Summary of mean fluorescence intensities of ICOS and Bcl-6 in different experiments are shown on the right. Statistical significance of differences among populations was calculated using a Friedman test followed by a Dunn's test (*p<0.05;**p<0.01, ***p<0.001).

Supplemental Figure 6.

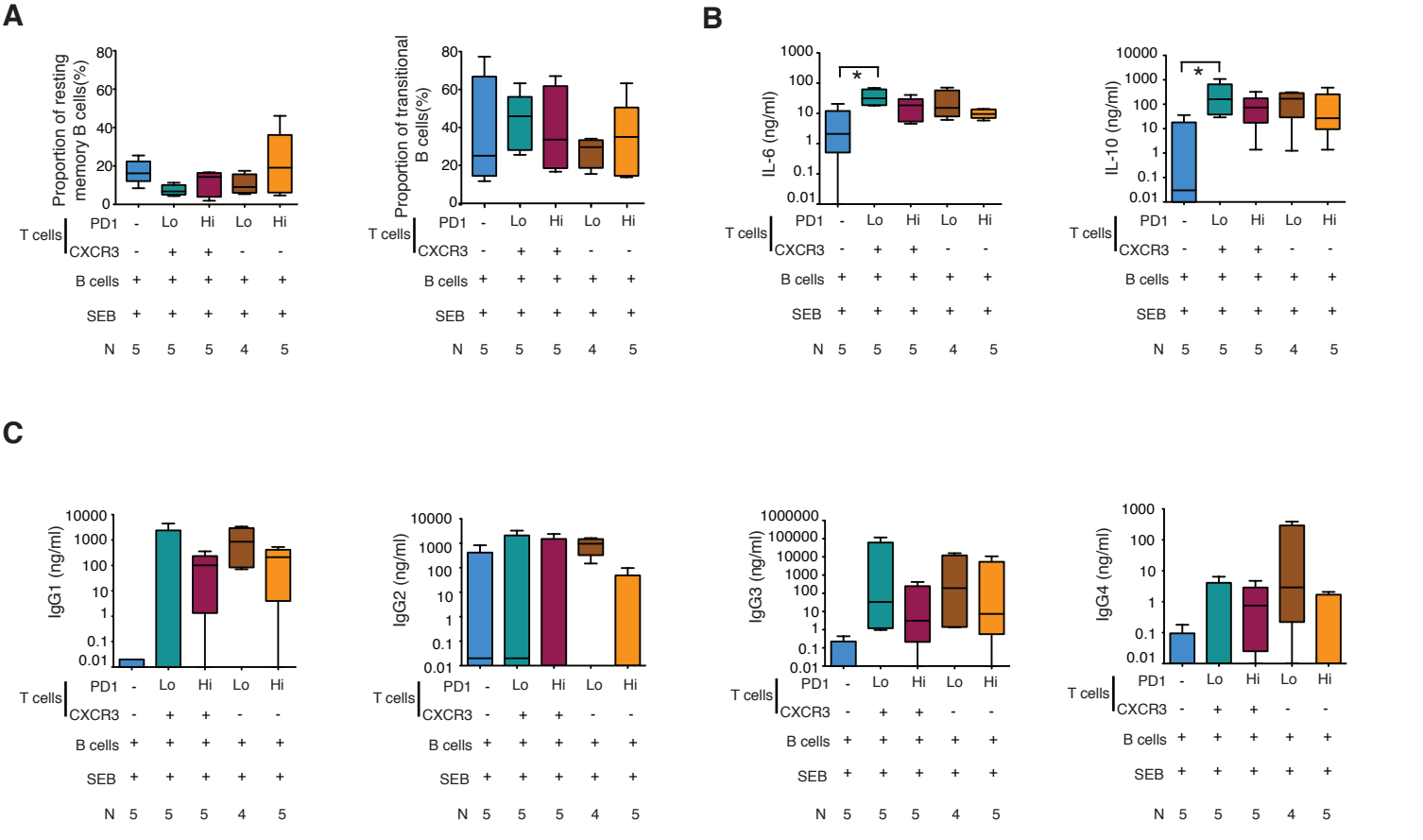

Supplemental Figure 6. Functional analysis of pTfh cells inducing B cell activation, cytokine secretion and production of Immunoglobulins. (A): Proportions of CD38$^-$ CD27$^+$ resting memory and CD38$^+$ CD27$^-$ transitional B cells on day 6 of co-culture with indicated pTfh populations. CXCR3$^+$ PD-1^{Lo} (n=5), CXCR3$^+$ PD-1^{Hi} (n=5), CXCR3$^-$ PD-1^{Lo} (n=4) and CXCR3$^-$ PD-1^{Hi} (n=5). (B-C): Luminex analysis of indicated cytokine (B) and IgG subclass (C) concentrations present in supernatants on day 6 in the indicated co-cultures of B cells alone or with CXCR3$^+$ PD-1^{Lo} (n=5), CXCR3$^+$ PD-1^{Hi} (n=5), CXCR3$^-$ PD-1^{Lo} (n=4) and CXCR3$^-$ PD-1^{Hi} (n=5) pTfh. Statistical significance among the 5 conditions was calculated using a Kruskal-Wallis test followed by Dunn's test (*p< 0.05).

Supplemental Figure 7

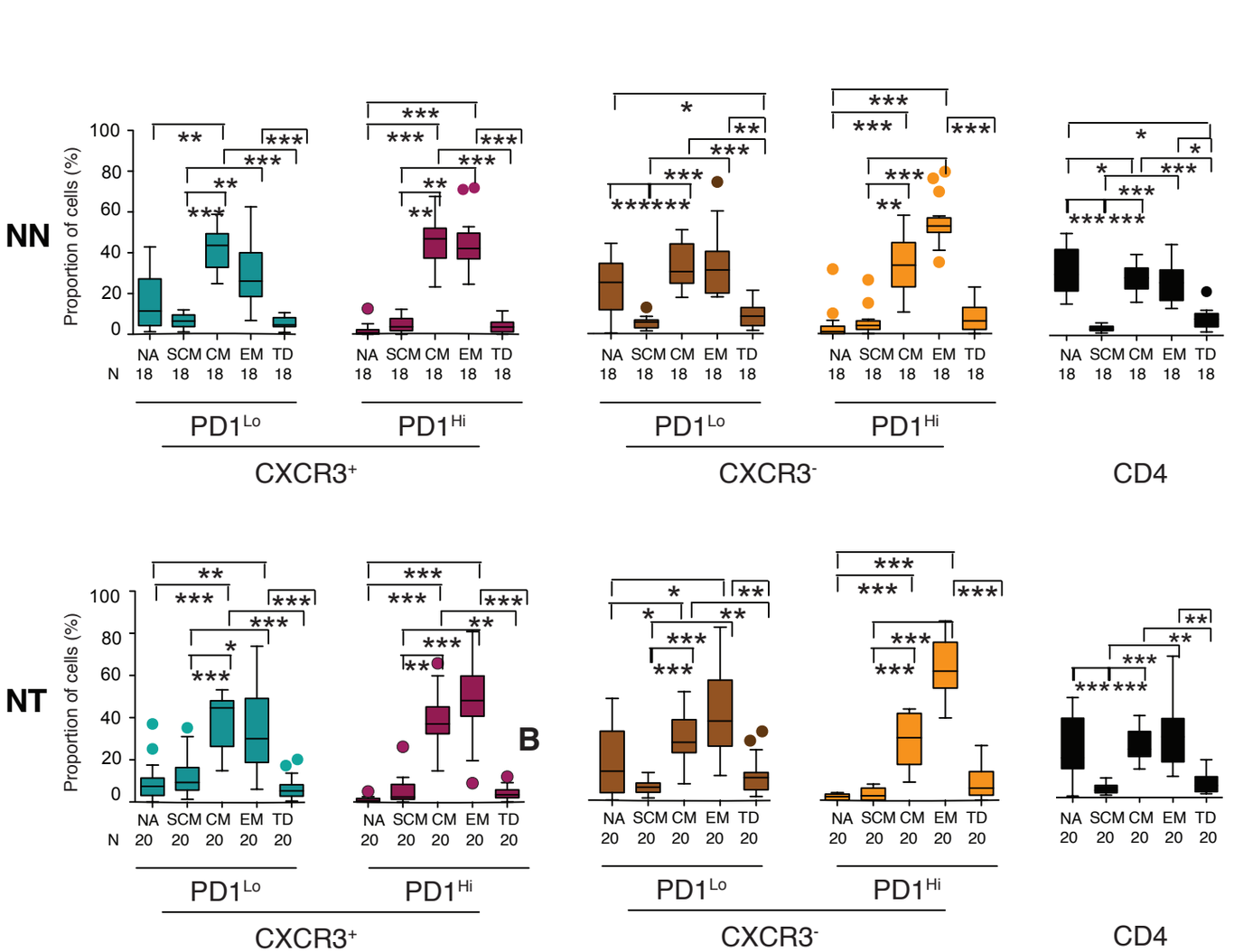

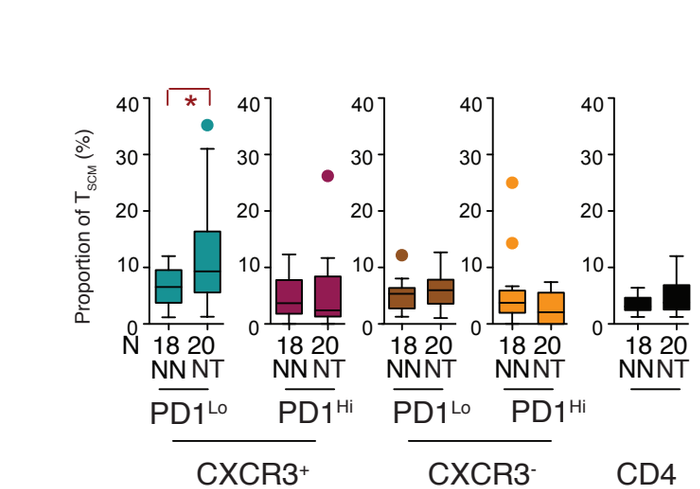

Supplemental Figure 7. Analysis of T cell memory subsets in circulating Tfh-like cell subpopulations from the blood of HIV-1 controller neutralizers and non neutralizers. (A): Proportions of naïve (NA), stem cell memory (SCM), central memory (CM), effector memory (EM), terminally differentiated (TD) cells defined by CCR7 vs CD45RO expression as shown in Figure 5A within CXCR3^{+} PD-1^{Lo} (green) and PD-1^{Hi} (garnet), CXCR3^{-} PD-1^{Lo} (brown) and PD-1^{Hi} (orange) and total CD4 T cells (CD4, black) from peripheral blood from HIV controller neutralizers (NT, n=18, ower row) and non-neutralizers (NN, n=20, upper row). Statistical differences in memory subset composition within each pTfh subpopulation were calculated using a Friedman test followed by a Dunn's test (*p<0.05; **p<0.01, ***p<0.001). (B): Distributions of SCM are also represented individually within each pTfh population comparing NN (n=18) and NT (n=20). Statistical differences in T_{SCM} proportions between HIV controller neutralizers and non neutralizers within each PD-1^{Lo} and PD-1^{Hi} pTfh subset was calculated using a one-tailed Mann Whitney test (*p<0.05,

Supplemental Figure 8.

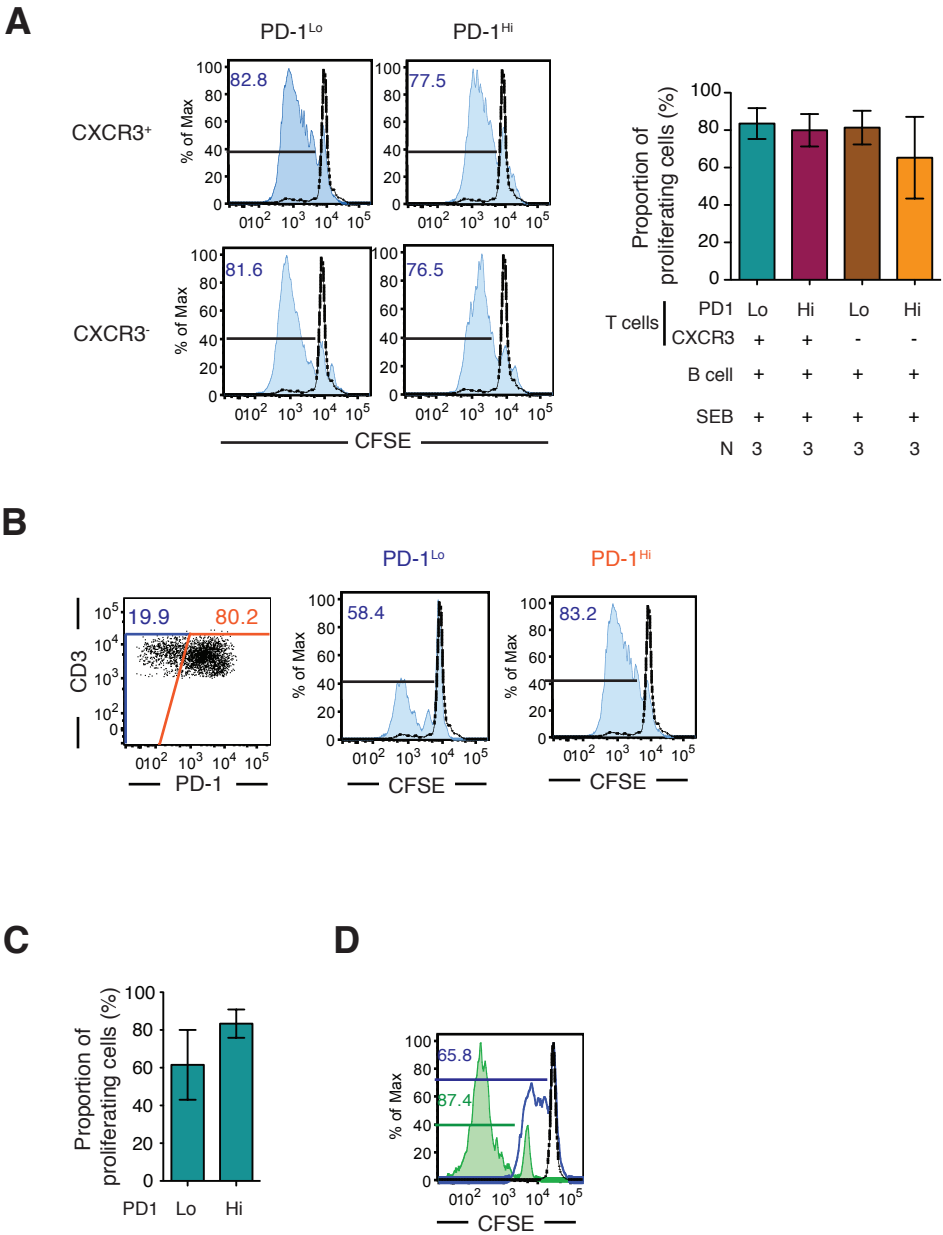

Supplemental Figure 8. Viability and proliferative capacity of different Tfh-like cell subpopulations from human blood. (A): Histograms (left panel) show representative flow cytometric analysis of CFSE dilution on sorted pTfh subpopulations on day 6 of culture with autologous B cells and SEB. Black dash lines reflect CFSE levels of control cells cultured with media alone. Numbers within histograms correspond to proportions of proliferating cells. Right panel summarizes proportions of proliferating CFSE^{Lo} cells in sorted pTfh subsets on day 6 (n=3). (B): Representative flow cytometric analysis showing CFSE dilution on gated PD-1^{Lo} and PD-1^{Hi} cells on day 6 of culture of sorted CXCR5^{+} CXCR3^{+} PD-1^{Lo} T cells with B cells and SEB. (C): summary the proportions of proliferating PD-1^{Lo} and PD-1^{Hi} cells in n=3 experiments. (D): Proliferative activity of CXCR5^{+} CXCR3^{+} PD-1^{Lo} cells assessed in serial culture experiments. PD-1^{Lo} cells isolated on day 6 are highlighted in blue; PD-1^{Lo} cells resorted on day 6 and cultured for six additional days are highlighted in green. Numbers in the histogram represent proportion of proliferating cells from corresponding populations. Unstimulated cells are shown in black dash line.